IRIS AperTO

UNIVERSITÀ DEGLI STUDI DI TORINO

AperTO - Archivio Istituzionale Open Access dell'Università di Torino

MET-driven resistance to dual EGFR and BRAF blockade may be overcome by switching from EGFR to MET inhibition in BRAF mutated colorectal cancer

This is the author's manuscript

Original Citation:

Availability:

This version is available http://hdl.handle.net/2318/1591711 since 2017-05-15T15:44:03Z

Published version:

DOI:10.1158/2159-8290.CD-16-0297

Terms of use:

Open Access

Anyone can freely access the full text of works made available as "Open Access". Works made available under a Creative Commons license can be used according to the terms and conditions of said license. Use of all other works requires consent of the right holder (author or publisher) if not exempted from copyright protection by the applicable law.

(Article begins on next page)

23 November 2024

IRIS AperTO

UNIVERSITÀ DEGLI STUDI DI TORINO

This is the author's final version of the contribution published as:

Pietrantonio, Filippo; Oddo, Daniele; Gloghini, Annunziata; Valtorta, Emanuele; Berenato, Rosa; Barault, Ludovic; Caporale, Marta; Busico, Adele; Morano, Federica; Gualeni, Ambra Vittoria; Alessi, Alessandra; Siravegna, Giulia; Perrone, Federica; Di Bartolomeo, Maria; Bardelli, Alberto; de Braud, Filippo; Di Nicolantonio, Federica. MET-Driven Resistance to Dual EGFR and BRAF Blockade May Be Overcome by Switching from EGFR to MET Inhibition in BRAF-Mutated Colorectal Cancer. CANCER DISCOVERY. 6 (9) pp: 963-971.
DOI: 10.1158/2159-8290.CD-16-0297

The publisher's version is available at:
http://cancerdiscovery.aacrjournals.org/cgi/doi/10.1158/2159-8290.CD-16-0297

When citing, please refer to the published version.

Link to this full text:
http://hdl.handle.net/

This full text was downloaded from iris - AperTO: https://iris.unito.it/

iris - AperTO

University of Turin's Institutional Research Information System and Open Access Institutional Repository

MET-driven resistance to dual EGFR and BRAF blockade may be overcome by switching from EGFR to MET inhibition in *BRAF* mutated colorectal cancer

Filippo Pietrantonio[1#*], Daniele Oddo[2,3,#], Annunziata Gloghini[4], Emanuele Valtorta[5], Rosa Berenato[1], Ludovic Barault[3], Marta Caporale[1], Adele Busico[4], Federica Morano[1], Ambra Vittoria Gualeni[4], Alessandra Alessi[6], Giulia Siravegna[2,3,7], Federica Perrone[4], Maria Di Bartolomeo[1], Alberto Bardelli[2,3], Filippo de Braud[1,8] & Federica Di Nicolantonio[2,3]

1- Medical Oncology Department, Fondazione IRCCS Istituto Nazionale dei Tumori, Milan, Italy;
2- Department of Oncology, University of Torino, 10060 Candiolo (TO), Italy;
3- Candiolo Cancer Institute-FPO, IRCCS, 10060 Candiolo (TO), Italy;
4- Department of Diagnostic Pathology and Laboratory Medicine, Fondazione IRCCS Istituto Nazionale dei Tumori, Milan, Italy;
5- Niguarda Cancer Center, Grande Ospedale Metropolitano Niguarda, 20162 Milan, Italy;
6- Nuclear Medicine Department, Fondazione IRCCS Istituto Nazionale dei Tumori, Milan, Italy;
7- FIRC Institute of Molecular Oncology (IFOM), 20139 Milan, Italy;
8- Department of Oncology, Università degli Studi di Milano, 20122 Milan, Italy

# Drs. Pietrantonio and Oddo contributed equally to this article

* To whom correspondence should be addressed:

Dr Filippo Pietrantonio,
Department of Medical Oncology, Medical Oncology Unit,
Fondazione IRCCS Istituto Nazionale dei Tumori,
Via Venezian 1, 20133 Milan, Italy
Phone: + 39-0223903807
E-mail: filippo.pietrantonio@istitutotumori.mi.it

Running title: Dual MET and BRAF inhibition in colon cancer

Keywords: BRAF, colorectal cancer, drug resistance, MET

Financial support

This work was supported by grants AIRC IG n. 17707 (FDN); Fondo per la Ricerca Locale (ex 60%), Università di Torino, 2014 (FDN). Partial support was also obtained by AIRC 2010 Special Program Molecular Clinical Oncology 5 per mille, Targeting resistances to molecular therapies in metastatic colorectal carcinomas, Project n. 9970 (AB); Fondazione Piemontese per la Ricerca sul Cancro-ONLUS 5 per mille 2010 e 2011 Ministero della Salute (AB, FDN); by European Community's Seventh Framework Programme under grant agreement no. 602901 MErCuRIC (A Bardelli, FDN).

Ludovic Barault was the recipient of a post-doctoral fellowship from Fondazione Umberto Veronesi in 2015 and of 'Assegno di Ricerca' from the University of Torino in 2016 .

Conflicts of interest disclosure: FP is a consultant/advisory board member for Roche, Amgen, Eli-Lilly, Bayer. MdB is a consultant/advisory board member for Eli-Lilly. FdB is a consultant/advisory board member for Roche, Novartis, Amgen, Celgene. The other authors declare no conflict of interest.

Word count (excluding references): 3,300

Number of tables/figures: 4

Abstract

A patient with metastatic *BRAF*-mutated colorectal cancer initially responded to combined EGFR and BRAF inhibition with panitumumab plus vemurafenib. Pre-existing cells with increased MET gene copy number in the archival tumor tissue likely underwent clonal expansion during treatment, leading to the emergence of *MET* amplification in the re-biopsy taken at progression. In *BRAF*-mutated colorectal cancer cells, ectopic expression of MET conferred resistance to panitumumab and vemurafenib, which was overcome by combining BRAF and MET inhibition. Based on tumor genotyping and functional *in vitro* data, the patient was treated with the dual ALK-MET inhibitor crizotinib plus vemurafenib, thus switching to dual MET and BRAF blockade, with rapid and marked effectiveness of such strategy. Although acquired resistance is a major limitation to the clinical efficacy of anticancer agents, the identification of molecular targets emerging during the first treatment may afford the opportunity to design the next-line of targeted therapies, maximizing patient benefit.

Statement of significance

MET amplification is here identified – clinically and pre-clinically - as a new mechanism of resistance to EGFR and BRAF dual/triple block combinations in *BRAF*-mutated colorectal cancer.
Switching from EGFR to MET inhibition, while maintaining BRAF inhibition, resulted in clinical benefit after the occurrence of MET-driven acquired resistance.

Introduction

Anticancer targeted therapies are hardly ever curative. Even in the setting of precision medicine, targeted agents fail to achieve prolonged responses in the vast majority of cases. Molecular characterization of tumor samples taken at relapse can inform about the mechanisms underlying acquired drug resistance and drive subsequent lines of therapy with the ultimate goal of prolonging disease control.

Combinations of anti-EGFR monoclonal antibodies and BRAF inhibitors (BRAFi), with or without other agents such as MEK or PI3K inhibitors, are emerging as an effective strategy to target *BRAF* V600E mutated metastatic colorectal cancer (CRC) (1-6). Therefore, *BRAF* mutations are evolving from a poor prognostic biomarker and a negative predictive factor for single-agents anti-EGFRs or BRAFi (7,8), to a positive selection marker for BRAFi-based dual or triple combinations. Nevertheless, the long-term efficacy of these targeted combinations is limited by the relatively rapid emergence of drug resistance (1, 2). Scant data are available about the molecular mechanisms underlying acquired resistance to targeted agents combinations in CRC. A previous study including three patients reported that acquired resistance to BRAFi in combination with either EGFR or MEK blockade in CRC cell lines and/or clinical samples is caused by the emergence of MAPK pathway molecular alterations including amplification of *KRAS* or mutated *BRAF* V600E, or mutations in *KRAS* or *MAP2K1* (9). However, the identification of the above mentioned molecular mechanisms has had no or very limited impact on the clinical management of individual *BRAF* mutant patients. In this work, we present how defining the spectrum of resistance mechanisms is critical to develop optimal subsequent treatment strategies aimed at prolonging survival. By genotyping a tissue biopsy, we identified the emergence of *MET* gene amplification as a mechanism of acquired drug resistance in a *BRAF* mutated metastatic CRC patient initially treated with the combination of panitumumab and vemurafenib. We describe how the combined data obtained by tumor molecular profiling and functional experiments in cell lines assisted therapeutic decision-making and offered the opportunity to deliver precision oncology.

Results

Emergence of *MET* gene amplification upon acquired resistance to panitumumab and vemurafenib

The patient clinical history is summarized in **Figure 1**. Approximately two years after multimodality treatment for *BRAF* V600E mutated, microsatellite stable mucinous rectal cancer, a 48-year-old man was diagnosed with pelvic relapse and liver metastases. First-line therapy with FOLFOXIRI obtained a disease stabilization lasting 9 months, indicating that intensive triplet treatment may achieve best outcomes in the poor-prognosis BRAF mutant mCRC patient subset. Following liver disease progression, the patient was given off-label treatment with panitumumab and vemurafenib according to a previously published phase II study (5). Within days of treatment start the patient symptoms improved and, after 2 months, a CT scan showed a partial response according to RECIST version 1.1 criteria **(Figure 2)**. Unfortunately, after 4 months, disease progression occurred (**Figure 2**). At this time, a liver tumor biopsy was obtained in order to investigate molecular mechanisms of acquired drug resistance. Molecular analyses were carried out in parallel both in pre-treatment primary tumor tissue and in post-treatment liver biopsy. Amplicon-based next-generation sequencing (NGS) of selected exons in 110 genes (Supplementary Table S1) did not identify nucleotide variants previously implicated in resistance to EGFR monoclonal antibodies or BRAF target therapies. In details, this analysis ruled out secondary mutations in likely candidate resistance genes including *EGFR*, *KRAS*, *NRAS* or *MAP2K1*.

Since amplicon-based NGS approaches do not allow accurate assessment of gene copy number changes, we performed immunohistochemical and *in situ* hybridization (ISH) analyses of HER2 and MET, as the activation of these genes had previously been associated with acquired resistance to EGFR monoclonal antibodies in CRC (10,11). No changes in HER2 expression or gene copy number status were observed (Supplementary Table S2). However, a marked difference was seen in MET expression (**Figure 2**). Analysis of the archival rectal sample showed heterogeneous MET immunostaining, with a strong membrane signal in about 50% neoplastic cells (H-score: 150), while the remaining cell population showed a weak to moderate membranous staining. Heterogeneity was also observed in *MET* gene copy number. By ISH (FISH and SISH) analyses, we estimated that the signals corresponding to the MET and CEP7 (chromosome seven α-centromeric) probes ranged from 1 to 8 (mean values of 3.52 and 2.89 for MET and CEP7, respectively), with a gene-to-chromosome ratio of 1.2, indicating chromosome 7 polysomy. However, in a small fraction of cells within the pre-treatment sample, the gene-to-chromosome ratio was ≥6, indicating subclonal *MET* gene

amplification (**Figure 2**, Supplementary Table S2). In the post-progression liver biopsy, MET was strongly expressed at the membrane level in about 90% neoplastic cells (H-score: 270). In this sample, *MET* copy number varied from 1 to 30 (mean 8.5), while CEP7 ranged from 1 to 16 (mean 3.24) with an overall gene-to-chromosome ratio of 2.62. At least 75% cells in the liver biopsy were found to carry *MET* gene amplification (**Figure 2**, Supplementary Table S2) (defined by a gene-to-chromosome ratio ≥6), indicating that dual EGFR-BRAF blockade had positively selected for *MET* amplified clones.

Since *MDM2* gene amplification has frequently been found to co-occur with *MET* genetic alteration in lung cancer (12), we assessed MDM2 gene copy number by ISH. This analysis suggested that dual BRAF and EGFR treatment had selected for *MDM2*-coamplified clones (**Supplementary Figure S1,** Panels **A-B**).

In order to investigate the prevalence of *MET* amplification in the context of BRAF mutant CRC, we performed *MET* ISH analysis on archival tumor tissue of 17 BRAF V600E advanced CRC samples. Three out of 17tumors (18%) from chemonaïve patients displayed *MET* amplified subclones (**Supplementary Figure S2,** Panels **A-D**).

Overexpression or amplification of MET confers resistance to targeted therapy combinations in BRAF mutant CRC cell lines

In order to assess whether MET overexpression alone is causally responsible for resistance to combinatorial vemurafenib and panitumumab treatment, we conducted *in vitro* forward genetic experiments. We took advantage of the *BRAF* mutant colorectal cancer cell line WiDr, which we had previously shown to be refractory to either single agent BRAF or EGFR inhibitors, but sensitive to their combination (13). Ectopic overexpression of MET in WiDr parental cells was able to confer resistance to combined vemurafenib and panitumumab by activating ERK signaling (**Figure 3A**) and sustaining proliferation (**Figure 3B**). Importantly, addition of the dual ALK-MET inhibitor crizotinib was able to restore sensitivity to combined vemurafenib and panitumumab in MET transduced cells (**Figure 3B**).

In vitro modeling of acquired resistance in cancer cell lines has proven effective in identifying resistance mechanisms that occur clinically (14,15). From a comprehensive effort aimed at defining the molecular landscape of resistance to targeted therapy combinations in *BRAF* mutant CRC cell lines (16), we detected the emergence of MET increased gene copy number and overexpression (**Figure 3C**) in a drug resistant WiDr subline (WiDr Res.) obtained by prolonged exposure of parental cells with cetuximab in association with the BRAF inhibitor encorafenib and the selective

PI3K-α inhibitor alpelisib (**Figure 3D**), a triplet regimen that is being tested in clinical trials (1). Functional experiments indicated that ectopic expression of MET in WiDr parental cells is able to confer resistance not only to combined BRAF and EGFR blockade, but also to the triplet regimen that includes PI3K inhibition (**Figure 3D**). WiDr resistant derivatives exhibited basal levels of activated RAS-GTP protein (**Supplementary Figure S3**) and constitutive phosphorylation of ERK despite combinatorial treatment with encorafenib+cetuximab+alpelisib (**Figure 3E**). WiDr resistant cells displaying *MET* amplification were clearly refractory to EGFR, BRAF and MEK targeted therapies, either as single agents or in combination (**Figure 3F**). Importantly, crizotinib alone showed no effects on the proliferation of WiDr resistant cells, whereas its combination with BRAF kinase inhibition by vemurafenib led to a marked decrease of cell viability over prolonged times (**Figure 3F**).

Altogether, these results directly underpin a causal relationship between *MET* amplification and resistance to targeted therapy combinations in *BRAF* mutant CRC and suggest a potential therapeutic strategy to overcome MET-mediated resistance.

Subsequent MET and BRAF targeted therapy overcomes clinical resistance to EGFR-BRAF dual block

The subsequent clinical history of the patient is again summarized in **Figure 1**. After 2 cycles of TAS-102, pelvic pain became severe and opioids were insufficient to achieve optimal symptom relief. Disease re-assessment with CT and FDG-PET/CT scans confirmed the rapid progression of the disease both loco-regionally (pelvic relapse with penis bulbs involvement and bilateral inguinal lymph nodes) and in the liver (**Figure 4A**). Prescription of regorafenib was contraindicated due to urinary fistula. In absence of further treatment options, based on tumor genotyping and preclinical data, and after ethical approval, combined MET and BRAF inhibition was considered as a rationale choice. Given the recent phase 1 data of crizotinib and vemurafenib combination (17), the patient started this combinatorial regimen in January 2016. After one week from treatment start, pelvic pain completely disappeared and the use of opioids was dramatically reduced. After 10-day treatment, a FDG-PET/CT scan showed an early and dramatic metabolic response (**Figure 4B**). Serum CA19-9 marker declined by >50% after only 2 weeks, and almost by 90% after 4 weeks (**Figure 1**). Treatment is still ongoing without significant toxicity.

Discussion

In this case study, we found for the first time that *MET* amplification and protein over-expression was the main molecular driver of clinical resistance to an anti-EGFR plus BRAFi combination. *MET*

amplification has been previously identified as a mechanism of resistance to targeted agents in other settings, including *BRAF* mutated melanoma treated with vemurafenib (10,18,19). *MET* amplification was also found in approximately 5%-20% of *EGFR*-mutated non-small cell lung cancers with acquired resistance to EGFR tyrosine kinase inhibitors (20) and in 10-20% *RAS/BRAF* wild-type CRC at progression upon anti-EGFR monoclonal antibodies (9). It was previously reported that *MET* amplification emerges in malignancies with pre-existing clones of *MET* amplified cells (21), which undergo positive selection during anti-EGFR based therapy in both NSCLC and CRC patients (10). The same seems to be true for the patient in our study, as molecular and histological analyses identified the presence of a subpopulation of *MET* amplified cells in the tumor sample before treatment with BRAF targeted therapy. The percentage of cells carrying *MET* gene copy amplification increased by at least five-fold in the post-treatment liver biopsy, indicating that dual EGFR-BRAF blockade had positively selected for *MET* amplified clones. We argue that the presence of a detectable fraction of pre-existing *MET* amplified cells has impacted negatively on the duration of response to dual EGFR and BRAF blockade, which was relatively short-lived. It is possible that in this case, combining upfront EGFR, MET and BRAF inhibition might have led to a more durable response and we suggest that future clinical studies should further investigate this aspect.

The proportion of *BRAF* mutant colorectal tumor samples co-harboring MET molecular alterations is unknown, but a large series of 1115 samples from any tumor types has previously reported that *MET* amplification was associated with a higher prevalence of *BRAF* mutation compared with non-amplified tumors (22). In our collection of 17 additional *BRAF* mutant CRC samples from chemonaive patients, we were able to find MET amplified subclones in three cases, Although none of the three patients actually received BRAF target agents, it is tempting to speculate that subclonal genetic diversity in these tumors could negatively influence the duration of response to BRAF combinatorial therapies due to likely clonal selection of MET amplification, On the other hand, it is possible that *MET* amplification could also be implicated in *de novo* resistance to target therapy combinations in BRAF mutant colorectal cancer. Pre-treatment tumor samples from non-responding patients enrolled in phase I-II studies with BRAFi combination therapies (2-6) will be essential to address this clinically relevant question.

Our preclinical experiments indicated that *MET* amplification emerged also as a driving mechanism of resistance in *BRAF* mutant CRC cells selected with cetuximab in combination with the BRAFi encorafenib and the PI3K inhibitor alpelisib. Ectopic overexpression of MET was able to confer resistance not only to panitumumab plus vemurafenib but also to the above clinically relevant triplet

which includes PI3K inhibition (1). This strongly suggests that MET activation is able to confer resistance to several BRAFi+EGFRi-based combinations, irrespective of the specific drugs used. Pharmacological data in CRC cells indicated that MET inhibition alone was ineffective to overcome resistance and that crizotinib should be combined with BRAF blockade to affect the proliferation of MET-overexpressing cells both in short-term and in long-term growth assays. This is consistent with what has been reported very recently in BRAF inhibitor resistant melanoma patient derived xenograft models, in which only combined vertical blockade of the pathway with MET and BRAF inhibitors was shown to induce durable regression in mice (23).

Based on preclinical modeling and functional characterization of MET aberrant signaling as a resistance mechanism to BRAF and EGFR dual blockade, the patient was treated with the combination of crizotinib and vemurafenib. The ALK inhibitor crizotinib is well known to bind also to MET tyrosine kinase domain and has shown clinical activity in MET amplified cancers (24,25). Moreover, recent phase 1 data showed that crizotinib may be safely combined with vemurafenib without occurrence of significant dose-limiting toxicities (17). Imaging revealed that switching from EGFR to MET blockade, while maintaining BRAF inhibition induced an extremely rapid and dramatic response following the initiation of treatment with crizotinib plus vemurafenib.

In this case, molecular analysis of a single-lesion biopsy did not identify any additional MAPK pathway molecular alterations beyond MET amplification that could eventually lead to treatment failure. Yet we admit that our strategy could have missed other resistance alterations occurring at subclonal level in the same lesion or as main drivers in other disease sites, since tumor heterogeneity may lead to the simultaneous selection of several inter- or intra-metastatic clones carrying different mechanisms of secondary resistance (26). However, metabolic response was observed across all disease sites, with *ex juvantibus* confirmation that MET might have been driving resistance in a relatively dominant and homogeneous fashion in this individual case of *BRAF*-mutated CRC. We acknowledge that early assessment with FDG-PET/CT may not be routinely accepted as an endpoint of treatment activity. However, the role of early metabolic response has gained robust evidence since the introduction of targeted therapies. In the era of precision medicine, the dramatic FDG-PET/CT response, necessarily coupled with the clinical and laboratory data, is indicative of immediate treatment benefit – even if longer follow up is needed to assess the duration of such benefit and potential emergence of further resistance mechanisms.

Extreme caution should be applied not to over-interpret the implications of this work. Indeed, we are well aware of the potential pitfalls of selecting a targeted therapy strategy based on the molecular profile of a single resistant lesion, as exemplified by recent case reports in CRC and breast cancer

patients (26, 27). Nevertheless, we believe that this case study may highly impact future research. In fact, specific targeting of MET-driven resistance to dual EGFR and BRAF block may lead to the design of biomarker-driven trials of second-line targeted therapy. Triple EGFR, MET and BRAF co-inhibition may also be investigated as additional strategy to prevent or overcome resistance in molecularly selected patients.

Methods

Patient Care and Specimen Collection

Tumor samples were collected in accordance with an Institutional Review Board–approved protocol, to which the patient provided written informed consent, and all studies were conducted in accordance with the Declaration of Helsinki. Targeted NGS on clinical specimens using was performed in the Department of Diagnostic Pathology and Laboratory Medicine at Fondazione IRCCS Istituto Nazionale dei Tumori, Milan, Italy. The patient's insurance company covered the cost of off-label combinatorial therapies (panitumumab+ vemurafenib; crizotinib+vemurafenib), to which the patient gave informed consent. CT scans were obtained as part of routine clinical care, while FDG-PET/CT scans were performed as part of an ancillary study protocol for patients receiving targeted treatments. The clinical course of the patient is summarized in **Figure 1**.

Next-generation sequencing

Next Generation Sequencing (NGS) analysis was performed as detailed in the Supplementary Methods and in Supplementary Table S2.

Immunohistochemistry

Immunohistochemistry (IHC) was performed on 3 μm formalin fixed paraffin-embedded (FFPE) tissue sections or on WiDr cytoclots. MET protein expression was detected by using a rabbit monoclonal anti-MET antibody (dilution 1:200; clone SP44, Spring Bioscience, Pleasanton, CA), directed against the synthetic peptide derived from C-terminus of human MET displaying membranous and/or cytoplasmic epitope. Other information is provided in the Supplementary Methods.

In situ hybridization (SISH and FISH)

MET gene status was assessed respectively by both SISH and FISH analyses scored blindly by two observers (A.G. and E.V.). Bright field dual-color SISH analysis was performed on 3 μm FFPE tissue sections by using the MET DNP Probe along with the Chromosome 7 DIG Probe (Ventana Medical

Systems) on a BenchMark Ultra Platform (Ventana Medical Systems) according to the manufacture's protocol. Dual color FISH analysis, both on metaphase chromosomes and interphase nuclei, obtained from WiDr cultured cells and on 3 μm FFPE tissue sections, was performed by using D7Z1 (7p11.1-q11.1) / c-MET (7q31.2) probes (Cytocell), respectively labelled with FITC and Texas Red. Procedure information is described in the Supplementary Methods.

For both SISH and FISH analyses the probes signals were counted in at least 100 non overlapping tumor cells nuclei from each case. Two independent molecular pathologists (A.G. and E.V.) scored the slides in a blinded fashion. *MET* gene amplification was defined as positive when: a) *MET*/CEP7 ratio was $\geq$ 2 or b) average number of *MET* signals per tumor cell nucleus was > 6.

SISH analyses for *MET* status were also performed on archival tumor tissue of 17 advanced colorectal tumors carrying mutant *BRAF* V600E diagnosed at Fondazione IRCCS Istituto Nazionale dei Tumori from 2012 to 2016.

Similarly, *HER2* gene amplification was defined as positive when: a) *HER2*/CEP17 ratio was $\geq$ 2 or b) average number of *HER2* signals per tumor cell nucleus was > 6.

Bright field dual-color SISH analysis was performed for *MDM2* by using the MDM2 DNP Probe along with Chromosome 12 DIG Probe (Ventana Medical Systems) on a BenchMark Ultra Platform (Ventana Medical Systems) according to the manufacture's protocol.

Cell lines and Treatments

WiDr parental cells were obtained from Dr René Bernards (Amsterdam, The Netherlands) in July 2011. The *KRAS* mutant SW480 cell line was purchased from ATCC (LGC Promochem) in January 2011. All cells were cultured at 37°C and 5% CO2 in RPMI 1640 (Invitrogen), supplemented with 10% fetal bovine serum, 2 mM L-glutamine and antibiotics (100 U/ml penicillin and 100 mg/ml streptomycin). The genetic identity of parental cell lines and their resistant derivatives was authenticated by short tandem repeat profiling (Cell ID System; Promega) at 10 different loci (D5S818, D13S317, D7S820, D16S539, D21S11, vWA, TH01, TPOX, CSF1PO and amelogenin) not fewer than 2 months before drug profiling or biochemical experiments. Cell lines were tested and resulted negative for Mycoplasma contamination with the VenorGeM Classic Kit (Minerva Biolabs). WiDr were made resistant by continuous drug exposure to the combination of cetuximab (5 μg/ml), encorafenib (1 μM) and alpelisib (0.5 μM). A detailed protocol of the drug proliferation assays is reported in the Supplementary Methods.

Western Blot analysis

Total cellular proteins was extracted by lysing cells in boiling Laemmli buffer (1% SDS, 50 mM Tris-HCl [pH 7.5], 150 mM NaCl). The following primary antibodies were used (all from Cell Signaling Technology, except where otherwise indicated): anti-MET (clone D1C2, 1:1000); anti-phospho MET (Tyr1234/1235, Cat.#3126; 1:1,000); anti-phospho p44/42 ERK (Thr202/Tyr204; 1:1,000); anti-p44/42 ERK (1:1,000); anti-phospho AKT (Ser473; 1:1,000); anti-AKT (1:1,000); HSP90 (Santa Cruz Biotechnology; 1:500).

Viral Infection

Lentiviral vector stock were produced by transient transfection of the pCCL-MET wild-type or lenti-control plasmid (a gift of Elisa Vigna, IRCCS, Candiolo, Turin) the packaging plasmid MDLg/pRRE and pRSV.REV, and the vesicular stomatitis virus (VSV) envelope plasmid pMD2.VSV-G (25, 2.5, 6.25 and 9 µg, respectively, for 15-cm dishes) in HEK-293T cells in presence of 1mM/L sodium butyrate (Sigma) and 10 ng/ml of Doxicicline. Cells were tranduced in six well plates (3 x 10^5 per well in 2 ml of medium) in the presence of polybrene (8 µg/ml) (Sigma).

Acknowledgments

The authors thank Prof. Silvia Giordano from the University of Torino for helpful scientific discussion. The authors also thank Elisa Vigna and Annalisa Lorenzato for providing lentiviral plasmids and Lara Fontani for help with lentiviral particles preparation. The Authors thank Chiara Volpi for support in ISH analyses, and Ilaria Bossi for data management.

References

1. Elez E, Schellens J, van Geel R, Bendell J, Spreafico A, Schuler M, et al. LBA-08 Results of a phase 1b study of the selective BRAF V600 inhibitor encorafenib in combination with cetuximab alone or cetuximab + alpelisib for treatment of patients with advanced BRAF-mutant metastatic colorectal cancer. Ann Onc. 2015;26:iv120.
2. Bendell JC, Atreya CE, André T, Tabernero J, Gordon MS, Bernards R, et al. Efficacy and tolerability in an open-label phase I/II study of MEK inhibitor trametinib (T), BRAF inhibitor dabrafenib (D), and anti-EGFR antibody panitumumab (P) in combination in patients (pts) with BRAF V600E mutated colorectal cancer (CRC). J Clin Oncol 32:5s, 2014 (suppl; abstr 3515).
3. Hong DS, Van Karlyle M, Fu S, Overman MJ, Piha-Paul SA, Kee BK, et al. Phase 1B study of vemurafenib in combination with irinotecan and cetuximab in patients with BRAF-mutated advanced cancers and metastatic colorectal cancer. J Clin Oncol 32:5s, 2014 (suppl; abstr 3516).
4. Tabernero J, Chan E, Baselga J, Blay JY, Chau I, Hyman DM, et al. VE-BASKET, a Simon 2-stage adaptive design, phase II, histology-independent study in nonmelanoma solid tumors harboring BRAF V600 mutations (V600m): Activity of vemurafenib (VEM) with or without cetuximab (CTX) in colorectal cancer (CRC). J Clin Oncol 32:5s, 2014 (suppl; abstr 3518^).
5. Yaeger R, Cercek A, O'Reilly EM, Reidy DL, Kemeny N, Wolinsky T, et al. Pilot trial of combined BRAF and EGFR inhibition in BRAF-mutant metastatic colorectal cancer patients. Clin Cancer Res. 2015;21:1313-20.
6. Corcoran RB, Atreya CE, Falchook GS, Kwak EL, Ryan DP, Bendell JC, et al. Combined BRAF and MEK Inhibition With Dabrafenib and Trametinib in BRAF V600-Mutant Colorectal Cancer. J Clin Oncol. 2015 Dec 1;33(34):4023-31. J Clin Oncol. 2015;33:4023-31.
7. Di Nicolantonio F, Martini M, Molinari F, Sartore-Bianchi A, Arena S, Saletti P, et al. Wild-type BRAF is required for response to panitumumab or cetuximab in metastatic colorectal cancer. J Clin Oncol. 2008;26:5705-12.
8. Pietrantonio F, Petrelli F, Coinu A, Di Bartolomeo M, Borgonovo K, Maggi C, et al. Predictive role of BRAF mutations in patients with advanced colorectal cancer receiving cetuximab and panitumumab: A meta-analysis. Eur J Cancer. 2015;51:587-94.
9. Ahronian LG, Sennott EM, Van Allen EM, Wagle N, Kwak EL, Faris JE, et al. Clinical Acquired Resistance to RAF Inhibitor Combinations in BRAF-Mutant Colorectal Cancer through MAPK Pathway Alterations. Cancer Discov. 2015;5:358-67.
10. Bardelli A, Corso S, Bertotti A, Hobor S, Valtorta E, Siravegna G, et al. Amplification of the MET receptor drives resistance to anti-EGFR therapies in colorectal cancer. Cancer Discov. 2013;3:658-73.
11. Yonesaka K, Zejnullahu K, Okamoto I, Satoh T, Cappuzzo F, Souglakos J, et al. Activation of ERBB2 signaling causes resistance to the EGFR-directed therapeutic antibody cetuximab. Sci Transl Med. 2011;3:99ra86.
12. Frampton GM, Ali SM, Rosenzweig M, Chmielecki J, Lu X, Bauer TM, et al. Activation of MET via Diverse Exon 14 Splicing Alterations Occurs in Multiple Tumor Types and Confers Clinical Sensitivity to MET Inhibitors. Cancer Discov. 2015;5:850-9.
13. Prahallad A, Sun C, Huang S, Di Nicolantonio F, Salazar R, Zecchin D, et al. Unresponsiveness of colon cancer to BRAF(V600E) inhibition through feedback activation of EGFR. Nature. 2012;483:100-3.
14. Engelman JA, Zejnullahu K, Mitsudomi T, Song Y, Hyland C, Park JO, et al. MET amplification leads to gefitinib resistance in lung cancer by activating ERBB3 signaling. Science. 2007;316:1039-43.
15. Russo M, Misale S, Wei G, Siravegna G, Crisafulli G, Lazzari L, et al. Acquired Resistance to the TRK Inhibitor Entrectinib in Colorectal Cancer. Cancer Discov. 2016;6:36-44.
16. Oddo D, Sennott EM, Barault L, Valtorta E, Arena S, Filiciotto G, et al. The molecular landscape of acquired resistance to targeted therapy combinations in BRAF mutant colorectal cancer. Cancer Res. [Epub ahead of print] doi 10.1158/0008-5472.CAN-16-0396

17. Kato S, Naing A, Falchook G, Holley VR, Velez-Bravo VM, Patel S, et al. Abstract 2689: Overcoming BRAF/MEK resistance using vemurafenib with crizotinib or sorafenib in patients with BRAF-mutant advanced cancers: phase I study. Cancer Research. 2015;75:2689-2689.
18. Straussman R, Morikawa T, Shee K, Barzily-Rokni M, Qian ZR, Du J, et al. Tumour micro-environment elicits innate resistance to RAF inhibitors through HGF secretion. Nature. 2012;487:500-4.
19. Wilson TR, Fridlyand J, Yan Y, Penuel E, Burton L, Chan E, et al. Widespread potential for growth-factor-driven resistance to anticancer kinase inhibitors. Nature. 2012;487:505-9.
20. Sequist LV, Waltman BA, Dias-Santagata D, Digumarthy S, Turke AB, Fidias P, et al. Genotypic and histological evolution of lung cancers acquiring resistance to EGFR inhibitors. Sci Transl Med. 2011;3:75ra26.
21. Turke AB, Zejnullahu K, Wu YL, Song Y, Dias-Santagata D, Lifshits E, et al. Preexistence and clonal selection of MET amplification in EGFR mutant NSCLC. Cancer Cell. 2010;17:77-88.
22. Jardim DL, Tang C, Gagliato Dde M, Falchook GS, Hess K, Janku F, et al. Analysis of 1,115 patients tested for MET amplification and therapy response in the MD Anderson Phase I Clinic. Clin Cancer Res. 2014;20:6336-45.
23. Krepler C, Xiao M, Spoesser K, Brafford PA, Shannan B, Beqiri M, et al. Personalized pre-clinical trials in BRAF inhibitor resistant patient derived xenograft models identify second line combination therapies. Clin Cancer Res. 2015.
24. Kwak EL, Ahronian LG, Siravegna G, Mussolin B, Godfrey JT, Clark JW, et al. Molecular Heterogeneity and Receptor Coamplification Drive Resistance to Targeted Therapy in MET-Amplified Esophagogastric Cancer. Cancer Discov. 2015;5:1271-81.
25. Ou SH, Kwak EL, Siwak-Tapp C, Dy J, Bergethon K, Clark JW, et al. Activity of crizotinib (PF02341066), a dual mesenchymal-epithelial transition (MET) and anaplastic lymphoma kinase (ALK) inhibitor, in a non-small cell lung cancer patient with de novo MET amplification. J Thorac Oncol. 2011;6:942-6.
26. Russo M, Siravegna G, Blaszkowsky LS, Corti G, Crisafulli G, Ahronian LG, et al. Tumor Heterogeneity and Lesion-Specific Response to Targeted Therapy in Colorectal Cancer. Cancer Discov. 2016;6:147-53.
27. Murtaza M, Dawson SJ, Pogrebniak K, Rueda OM, Provenzano E, Grant J, et al. Multifocal clonal evolution characterized using circulating tumour DNA in a case of metastatic breast cancer. Nat Commun. 2015;6:8760.

Figure Legends

Figure 1. Summary of patient clinical history.

The clinical course of the patient with colorectal cancer is summarized, with serum cancer antigen 19-9 tumor marker levels shown throughout treatment (green line). Shaded boxes indicate periods of administration of the indicated chemotherapeutic agents. Blue vertical lines indicate timing of tumor specimen acquisition from surgical procedures or biopsy, as well as dates of tumor assessment by either CT scan or FDG-PET/CT scan.

Figure 2. MET amplification is selected for in a BRAF mutant CRC biopsy from a patient who developed resistance to combined BRAF and EGFR targeted treatments

In panel A, baseline CT scan prior to start of panitumumab and vemurafenib, showing liver involvement; in panel B, partial response to treatment according to RECIST 1.1 at week 8; in panel C, progressive disease during treatment at week 16.

In panel A1-4 and C1-4: analyses performed on archival surgical specimen and on post-progression liver rebiopsy, respectively. A1-C1. Conventionally stained section using Hematoxylin & Eosin, showing poorly differentiated carcinoma of the rectum (A1) and liver metastasis (C1) (A1-C1, original magnification x20); A2-C2. Immunohistochemical detection of MET protein. The primary tumor displays heterogeneous immunostaining ranging from weak to moderate (at the center) intensity (A2). Metastatic tumor cells display homogeneous, strong immunostaining (C2) (A2-C2, original magnification X20); A3-C3. Dual color bright field in situ hybridization (ISH) for *MET* gene (black dots) and CEP7 (red dots). The primary tumor, though not amplified, display heterogeneous, *MET* gene copy number, ranging from 1 to 7 (A3). Metastatic tumors cells contain high *MET* gene copy number (ranging from 2 to 20) featuring *MET* gene amplification (C3) (A3-C3, original magnification X20). A4-C4. Dual color FISH analysis using D7Z1 (7p11.1-q11.1) / c-MET (7q31.2) probes (Cytocell), respectively labeled with FITC and Texas Red. The primary tumor (A4, original magnification x100) shows heterogeneous, MET gene copy number, ranging from 1 to 8, while metastatic tumors cells (C4, original magnification x100) contain high *MET* gene copy number (ranging from 2 to 30) featuring *MET* gene amplification.

Figure 3. MET overexpression or gene amplification confers resistance to targeted therapy combinations in BRAF mutant CRC cells. A, BRAF mutant WiDr cells were transduced with either control (empty) or MET–expressing lentiviral vectors. Cells were then treated with vemurafenib (2 μM), panitumumab (5 μg/ml) and their combination for 5 hours prior to protein

extraction and Western blotting with total MET, phosphorylated–MET (Tyr 1234-1235), total AKT, phosphorylated-AKT (Ser473), total ERK1/2 and phosphorylated-ERK1/2 (Thr 202 /Tyr 204) antibodies. HSP90 was included as a loading control. **B,** After 96-hour treatment with panitumumab (5 μg/ml), vemurafenib (1 μM), crizotinib (0.3 μM) or their combinations, the viability of empty or lenti-MET transduced cells was assessed by relative ATP content measurement. Results represent mean ± SD of at least 2 independent observations, each performed in triplicate. ** P<0.01; *** P<0.001 Bonferroni's adjusted ANOVA *p* values; **C**, FISH analysis and immunohistochemistry (IHC) showing *MET* gene amplification (top) and MET protein overexpression (bottom), respectively, in WiDr resistant derivatives (WiDr res) generated from WiDr parental (WiDr par) cells after several weeks' continuous treatment with the triple combination encorafenib+cetuximab+alpelisib; MET (7q31)–specific probe is labeled with Texas red, whereas chromosome 7 centromeric probe D7Z1 (7p11.1–q11.1) is marked in green. FISH, original magnification 100×; IHC, original magnification ×40; **D**, Cell viability by ATP assay of WiDr parental cells and resistant derivatives, as well as WiDr transduced with MET after treatment for 96 hours with the indicated molar concentrations of encorafenib in association with constant 5 μg/ml cetuximab and 0.5 μM alpelisib. Results represent mean ± SD of at least 2 independent observations, each performed in triplicate. **E**, WiDr parental cells and their *MET* amplified subline with acquired resistance to the triple combination encorafenib+cetuximab+alpelisib were treated with the combination of encorafenib (0.4 μM), cetuximab (5 μg/ml) and alpelisib (1 μM) for 5 hours prior to protein extraction and Western blotting with the indicated antibodies. **F**, Long-term colony forming assay of *MET* amplified encorafenib+cetuximab+alpelisib resistant WiDr cells treated for 12-14 days in the absence or presence of panitumumab (EGFRi, 5 μg/ml), trametinib (MEKi, 10 nM), crizotinib (0.3 μM), vemurafenib (BRAFi, 1.5 μM) or their combinations. Results are representative of at least 2 independent observations.

Figure 4. 18F-FDG PET/C T scans at baseline and 10 days after the start of combination treatment with crizotinib and vemurafenib. Panel **A** (coronal and axial fused images) shows liver metastases (red arrows) and pelvic/inguinal lymph node involvement (white arrows) at baseline. Panel **B** (coronal and axial fused images) shows marked metabolic response at all sites of disease.

Figure 1

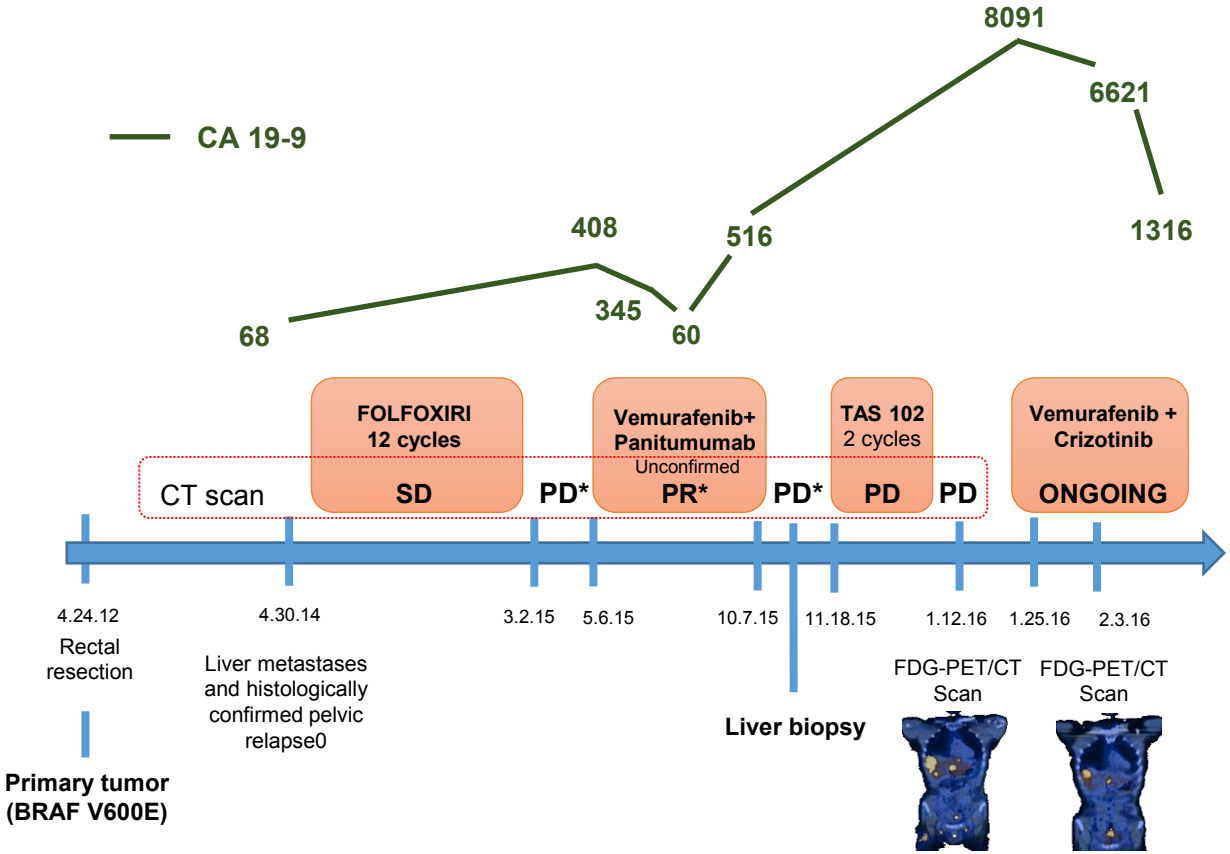
CA 19-9
68
408
345
60
516
8091
6621
1316
FOLFOXIRI
12 cycles
SD
Vemurafenib+
Panitumumab
Unconfirmed
PR*
TAS 102
2 cycles
PD
Vemurafenib +
Crizotinib
ONGOING
CT scan
PD*
PD*
PD
4.24.12
Rectal
resection
4.30.14
Liver metastases
and histologically
confirmed pelvic
relapse0
3.2.15
5.6.15
10.7.15
11.18.15
1.12.16
1.25.16
2.3.16
Primary tumor
(BRAF V600E)
Liver biopsy
FDG-PET/CT
Scan
FDG-PET/CT
Scan

Figure 2

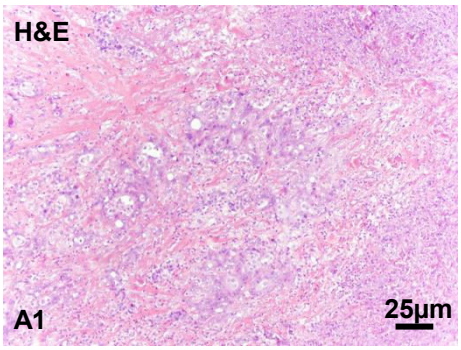

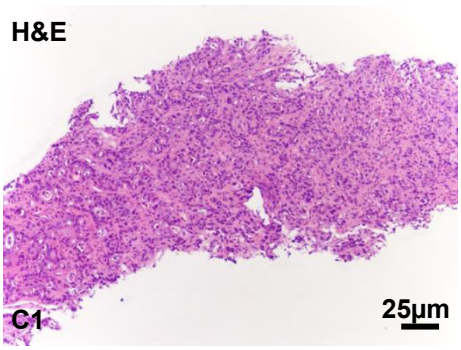

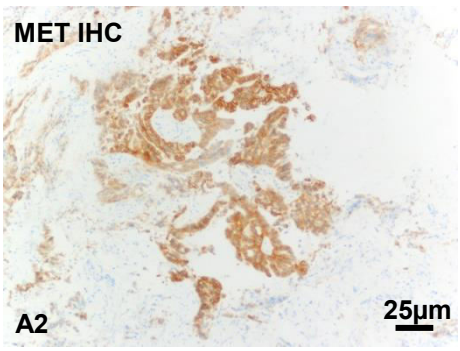

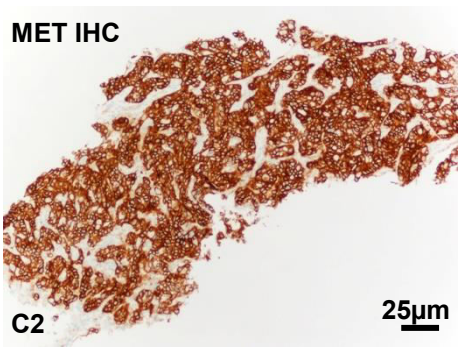

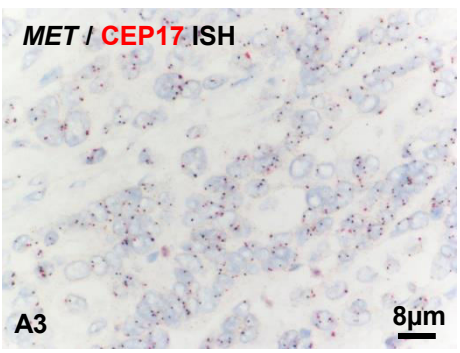

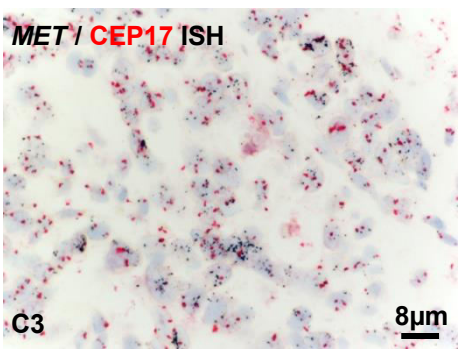

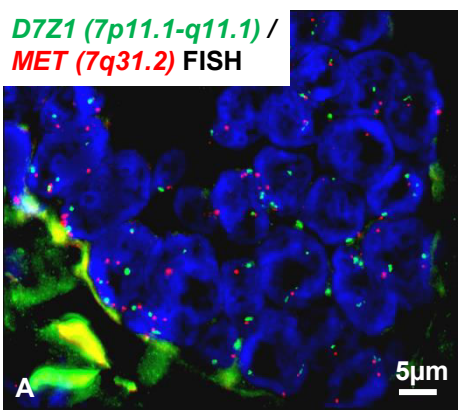

Pre-treatment

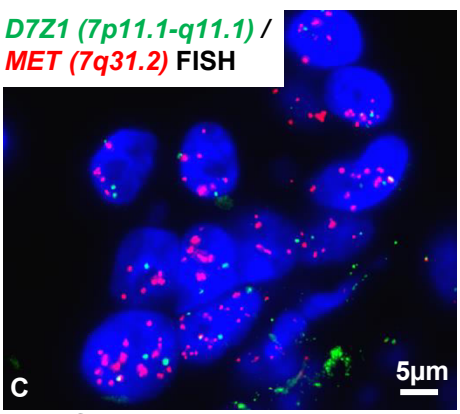

After panitumumab +vemurafenib

Figure 3

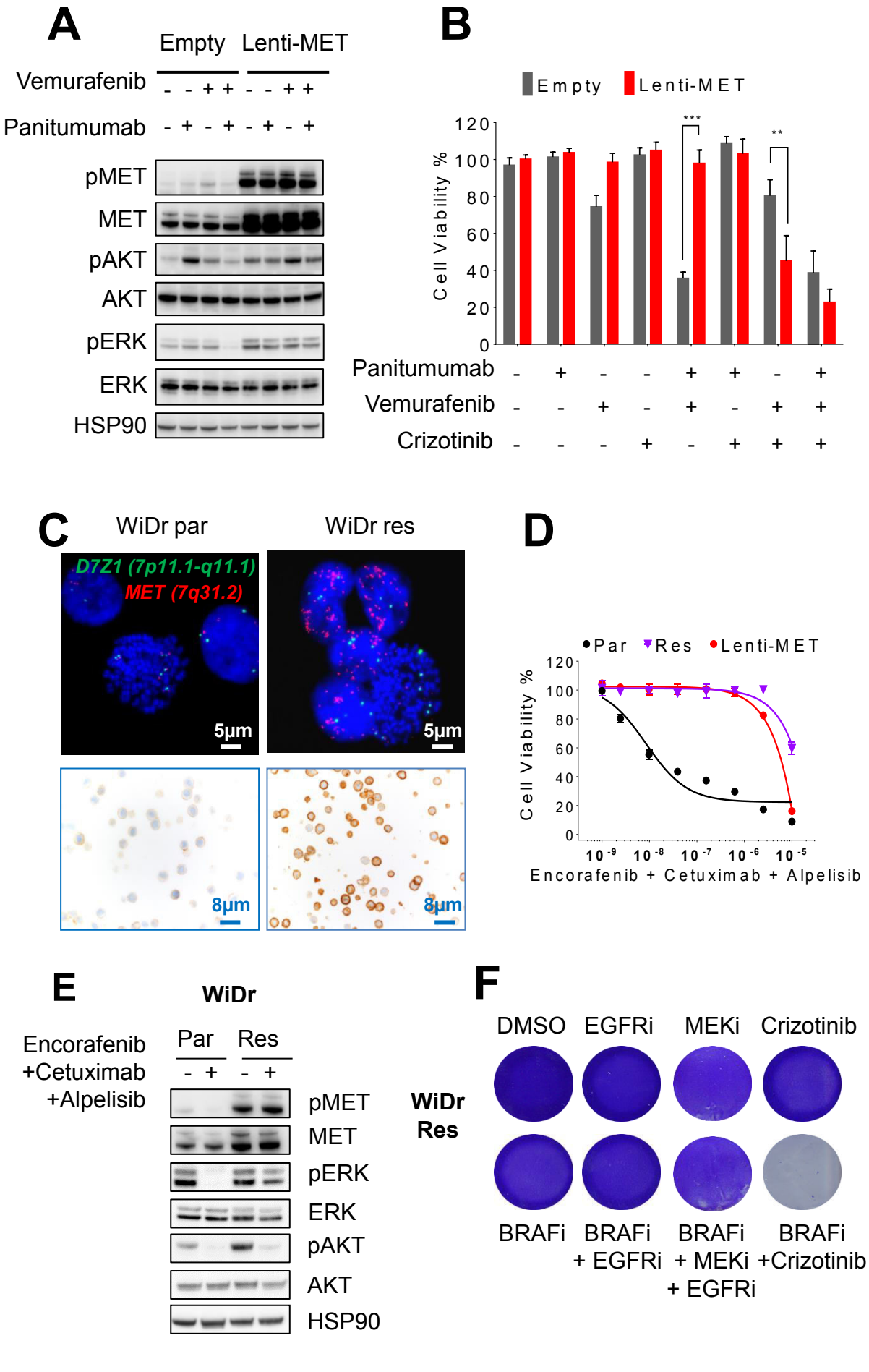
A
Empty
Lenti-MET
Vemurafenib
- - + + - - + +
Panitumumab
- + - + - + - +
pMET
MET
pAKT
AKT
pERK
ERK
HSP90
B
Empty
Lenti-MET
Cell Viability %
120
100
80
60
40
20
0
***
**
Panitumumab - + - - + + - +
Vemurafenib - - + - + - + +
Crizotinib - - - + - + + +
C
WiDr par
WiDr res
D7Z1 (7p11.1-q11.1)
MET (7q31.2)
5µm
5µm
8µm
8µm
D
Par
Res
Lenti-MET
Cell Viability %
120
100
80
60
40
20
0
10 -9
10 -8
10 -7
10 -6
10 -5
Encorafenib + Cetuximab + Alpelisib
E
WiDr
Encorafenib
+Cetuximab
+Alpelisib
Par
Res
- + - +
pMET
MET
pERK
ERK
pAKT
AKT
HSP90
F
DMSO
EGFRi
MEKi
Crizotinib
WiDr Res
BRAFi
BRAFi + EGFRi
BRAFi + MEKi + EGFRi
BRAFi +Crizotinib

Figure 4

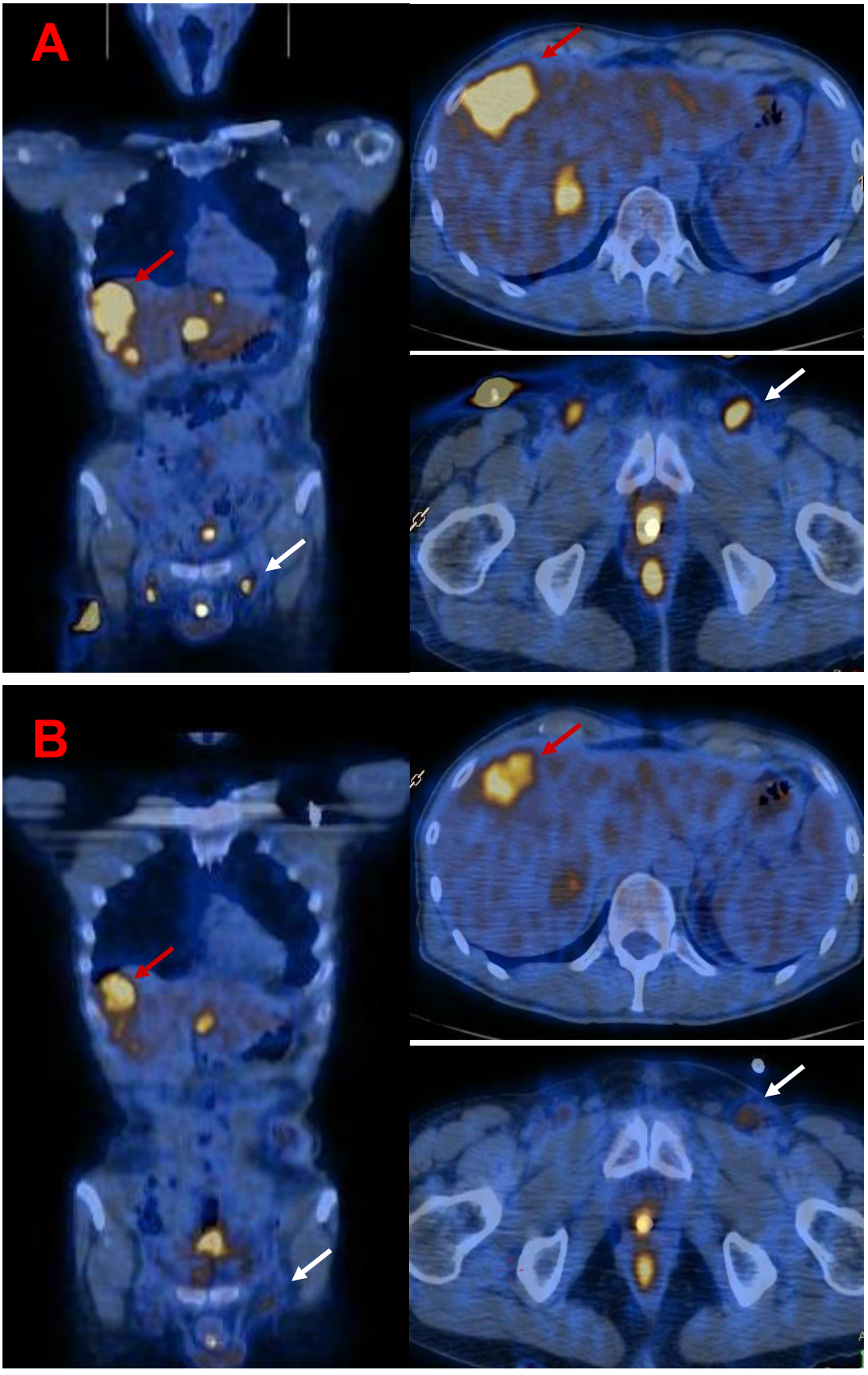

MET-driven resistance to dual EGFR and BRAF blockade may be overcome by switching from EGFR to MET inhibition in *BRAF* mutated colorectal cancer

Supplementary Figures

Supplementary Fig.S1

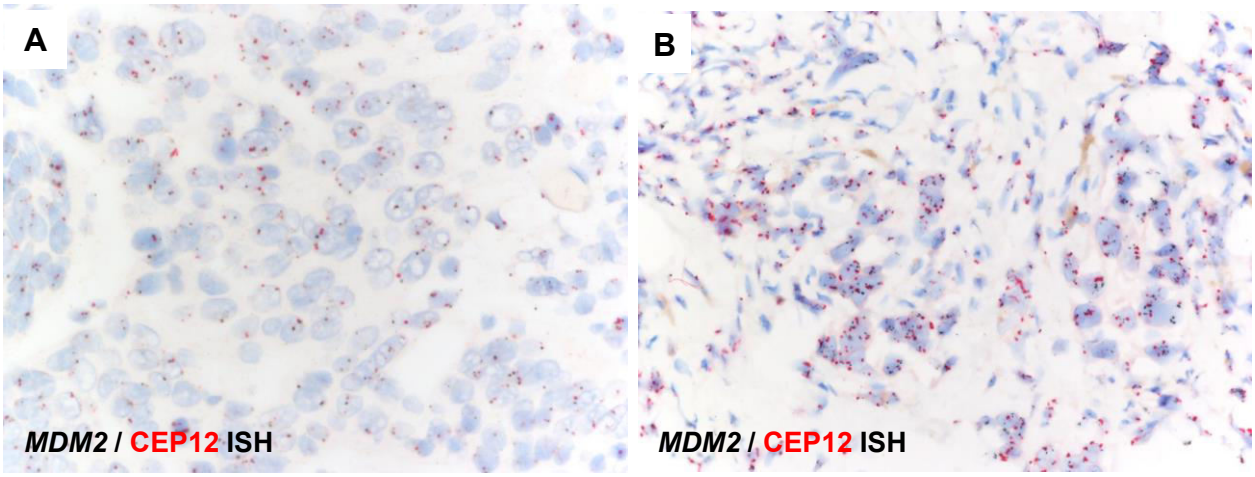

Supplementary Fig.S2

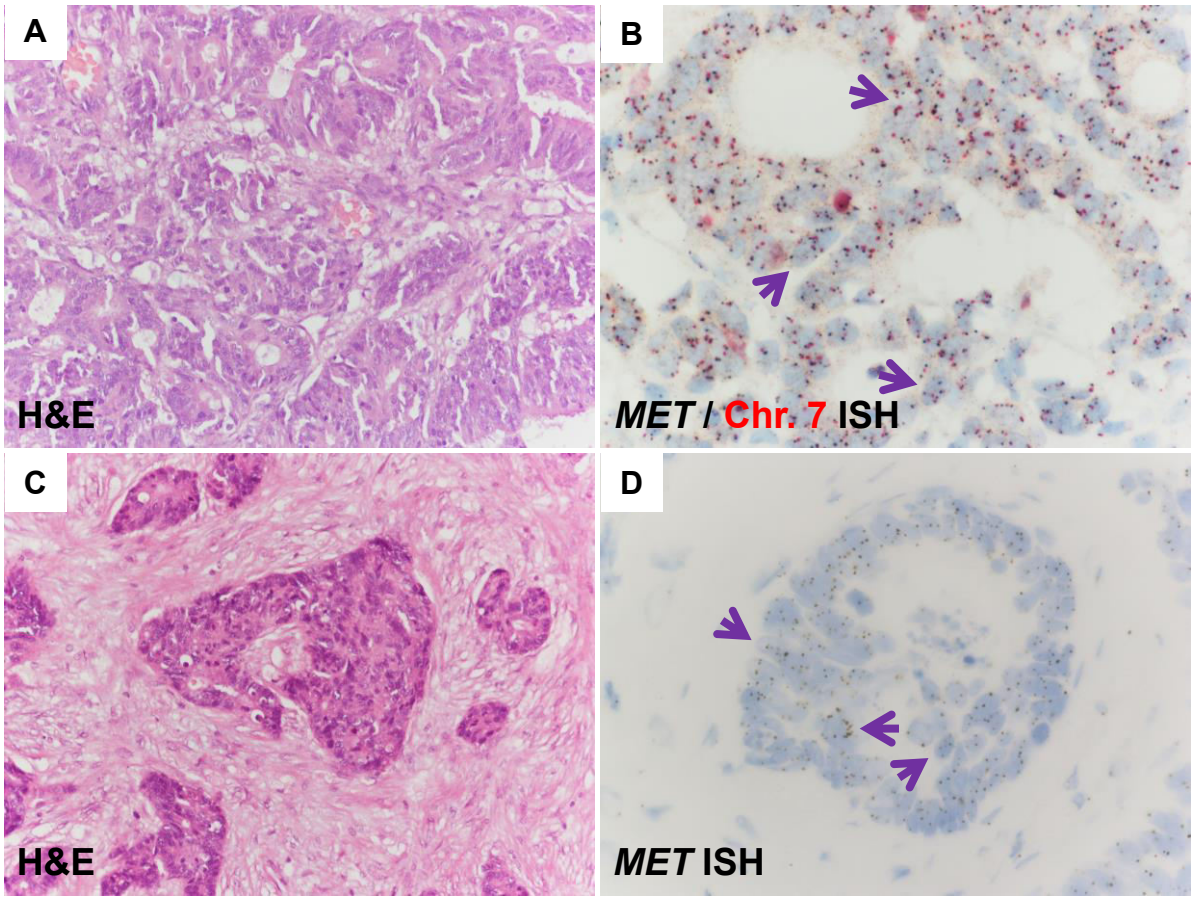

Supplementary Fig.S3

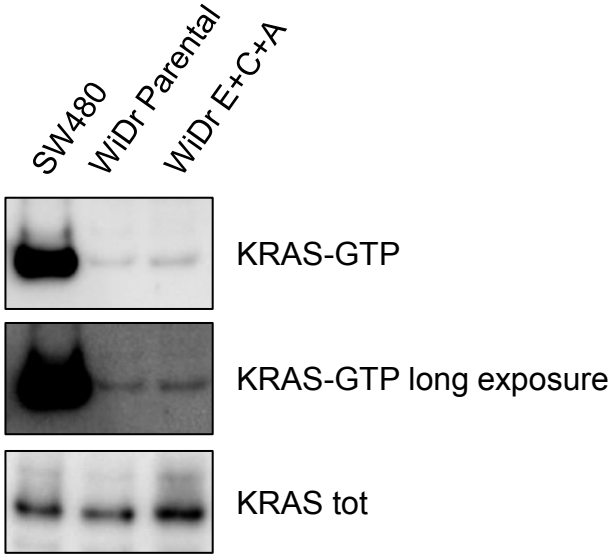

Legend to Supplementary Figures

Supplementary Figure S1. Copy number increase of *MDM2* gene at progression after vemurafenib+panitumumab.

In panel **A** and **B**: analyses performed on archival surgical specimen and on post-progression liver rebiopsy, respectively. Dual color bright field in situ hybridization (ISH) for *MDM2* gene (black dots) and CEP12 (chromosome twelve α-centromeric, red dots). In baseline tumor tissue, the signals corresponding to the MDM2 and CEP12 probes ranged from 2 to 5 (mean values of 3.5 and 3.3 for MDM2 and CEP12, respectively), with a gene-to-chromosome ratio of just over 1, indicating absence of gene amplification. However, in a small fraction of cells (5%) within the pre-treatment sample the *MDM2* gene copy number was ≥5. In the post-progression tumor biopsy, MDM2 copy number varied from 3 to 16 (mean 7.2) while CEP12 ranged from 1 to 8 (mean 3.4). At least 75% cells in the post-treatment liver biopsy were found to carry ≥5 *MDM2* gene copy number and the gene-to-chromosome ratio was >2. Original magnification X20.

Supplementary Figure S2. A-D. Representative examples of colorectal carcinomas bearing BRAF mutations and *MET* gene copy number gain.

A Hematoxylin & Eosin staining of a poorly differentiated colon carcinoma. **B** Dual color bright field ISH for *MET* gene (black dots) and CEP7 (red dots) of case in panel A. Tumor cells contain *MET* gene copy number (ranging from 2 to 7; mean: 4.2) and Chromosome 7 signals (ranging from 2 to 5; mean: 3.4). Interestingly, 38% of neoplastic cells featured ≥ 5 *MET* gene copy number. **C** Hematoxylin & Eosin staining of a pancreatic lesion from an intestinal adenocarcinoma. **D** Single color bright field ISH for *MET* gene (black dots) of case in panel C. Tumor cells contain *MET* gene copy number (ranging from 4 to 11; mean: 5.4). Up to 77% of tumor cells contained ≥ 5 *MET* gene copy number. Arrows indicate neoplastic cells with high *MET* gene copy number.

Supplementary Figure S3. Untreated WiDr parental cells exhibit similar levels of activated RAS-GTP protein compared to their MET-amplified resistant derivatives treated with encorafenib+cetuximab+alpelisib (E+C+A). Whole-cell extracts were subjected to pull-down of active KRAS-GTP using the GST-RAF1 Ras-binding domain. Lysate of SW480 colorectal cancer cells carrying a *KRAS* G12V mutation is loaded as a positive control.

Supplementary Data

MET-driven resistance to dual EGFR and BRAF blockade may be overcome by switching from EGFR to MET inhibition in *BRAF* mutated colorectal cancer

Filippo Pietrantonio, Daniele Oddo, Annunziata Gloghini, Emanuele Valtorta, Rosa Berenato, Ludovic Barault, Marta Caporale, Adele Busico, Federica Morano, Alessandra Alessi, Giulia Siravegna, Federica Perrone, Andrea Sartore-Bianchi, Salvatore Siena, Maria Di Bartolomeo, Alberto Bardelli, Filippo de Braud, Federica Di Nicolantonio

Supplementary Methods …….……page 2

Supplementary Table S1……..page 5

Supplementary Table S2……....page 30

Supplementary Methods

Preparation of cytoclots

WiDr cytoclots were prepared by pelleting up to $50x10^6$ cells and re-suspending them in 1% agar, followed by polymerization in dry ice for a few seconds, fixation in paraformaldehyde 4% and ethanol 70% at +4°C for 4 hours, and final embedding in paraffin wax.

Immunohistochemistry

IHC was carried out on a BenchMark Ultra Platform (Ventana Medical Systems, Tucson, AZ) by using the OptiviewDAB Detection Kit (Ventana Medical Systems). MET IHC was evaluated according to a semi-quantitative assessment (H-score) which combines staining intensity (scored from 0 to 4) with the percentage of positive cells (scored 0–100%). Each individual intensity level is multiplied by the percentage of cells and all values are added to obtain the final IHC score, ranging from 0 to 400. Scores from 0 to 200 are considered negative/low expression and scores from 201 to 400 are considered positive/high expression.

HER2 protein expression was evaluated by using the anti-human c-erbB-2 A0485 polyclonal antibody (dilution 1:1500; Dako Denmark A/S, Glostrup, Denmark) on a DakoAutostainer Plus by using the EnVision® FLEX+ (Dako) detection system. HER2 immunoreactivity was evaluated according to previously described scoring systems (1).

Fluorescence *In Situ* Hybridization

For both cell lines and clinical samples dehydration was carried out in ethanol series (70%, 90%, 100%), followed by 3 washes (5' each) and air drying. Probes and target DNA were co-denatured for 5 min at 75 °C and then hybridized overnight at 37 °C. Slides were washed with washing solution I (0.4x SSC, 0.3% NP-40) for 5 min at 73 °C, for 1 min with washing solution II (2x SSC/0.1% NP-40) at room temperature (Abnova) and finally counterstained with 4′,6-diamidino-2-phenylindole (DAPI). FISH signals were evaluated with a Zeiss Axioscope Imager.Z1 (Zeiss) equipped with single and triple band pass filters.

Next-generation sequencing

DNA extraction was performed as previously described (2). Next Generation Sequencing (NGS) analysis was performed by using small genomic DNA samples (20 ng/μl) and the Ion-Torrent™ Personal Genome Machine platform (Life Technologies-Thermo Fisher Scientific, USA). A

detailed description of the applied T-NGS procedures has been previously published (2). For this study, we used two custom panels, the first of which designed to amplify 3358 amplicons (246,15 kb) from 110 oncogenes and tumor suppressor genes recurrently mutated in human cancers and a second custom panel to analyze 26 amplicons (2,77 kb) corresponding to the EGFR extra-cellular region (exons from 1 to 14), as detailed in Supplementary Table S1.

Drug proliferation assays

Vemurafenib, trametinib and encorafenib were purchased from Sequoia Chemicals; crizotinib and alpelisib were from Selleckchem and ChemieTek respectively. The EGFR targeted monoclonal antibodies cetuximab and panitumumab were obtained from the Pharmacy at Ospedale Niguarda, Milan. Cell proliferation experiments were carried out in 96-well plates in triplicate. A total of 2,000 cells/well were seeded in 100 µl complete growth medium. At 24 hours post-seeding, 100 µl of serum-free medium with or without cetuximab or panitumumab (both 5 µg/ml) was manually added to the cells. All other drugs were added directly on the plate by TECAN D300e digital dispenser (HP). After 72-96 hours' treatment cell viability was assessed by ATP content using CellTiter-Glo Luminescent Assay (Promega). Viability was normalized as a percentage of control untreated cells. Data from growth-inhibition assays were plotted using the nonlinear regression curve fit modelling from GraphPad Prism-6 (GraphPad Software). For long-term proliferation assays, cells were seeded in 6-well plates (20,000 cells/well) and cultured in the absence and presence of drugs as indicated. Wells were fixed with 4% paraformaldehyde and stained with 1% crystal violet-methanol solution (Sigma-Aldrich) after 12-14 days. All assays were performed independently at least two times.

RAS Activation Assay

GST-RAF1-RAS-binding domain fusion protein expression was induced in Escherichia coli for 3 hr at 30°C with 0.2 mM isopropyl-1-thioβ-D-galactopyranoside. Bacterial pellet was resuspended in lysis buffer (PBS, 1 mM PMSF, 5 mM β-mercaptoethanol, mixture of protease inhibitors) and sonicated. The soluble GST tagged proteins were isolated with glutathione agarose beads. Forty micrograms of purified proteins were then incubated with 2 mg of whole-cell cleared lysate. The complexes were collected by centrifugation and analyzed by western blot using an anti-KRAS monoclonal antibody (clone 3B10-2F2; Sigma-Aldrich; 1:500). Twenty microgram of total lysates from the above cells were immunoblotted with anti-KRAS antibody as a loading control.

Supplementary References

1. Valtorta E, Martino C, Sartore-Bianchi A, Penaullt-Llorca F, Viale G, Risio M, et al. Assessment of a HER2 scoring system for colorectal cancer: results from a validation study. Mod Pathol. 2015;28:1481-91.
2. Pelosi G, Fabbri A, Papotti M, Rossi G, Cavazza A, Righi L, et al. Dissecting Pulmonary Large-Cell Carcinoma by Targeted Next Generation Sequencing of Several Cancer Genes Pushes Genotypic-Phenotypic Correlations to Emerge. J Thorac Oncol. 2015;10:1560-9.

Supplementary Table S1. List of genes and exons analyzed by targeted next-generation sequencing.

GENE-EXON	Reference	Chromosome	CHR_Start	CHR_End	STRAND
ARID1A	GRCh37/hg19	chr1	27022890	27024036	+
ARID1A	GRCh37/hg19	chr1	27056137	27056359	+
ARID1A	GRCh37/hg19	chr1	27057638	27058100	+
ARID1A	GRCh37/hg19	chr1	27059162	27059288	+
ARID1A	GRCh37/hg19	chr1	27087342	27087592	+
ARID1A	GRCh37/hg19	chr1	27087870	27087969	+
ARID1A	GRCh37/hg19	chr1	27088638	27088815	+
ARID1A	GRCh37/hg19	chr1	27089459	27089781	+
ARID1A	GRCh37/hg19	chr1	27092707	27092862	+
ARID1A	GRCh37/hg19	chr1	27092943	27093062	+
ARID1A	GRCh37/hg19	chr1	27094276	27094495	+
ARID1A	GRCh37/hg19	chr1	27097605	27097822	+
ARID1A	GRCh37/hg19	chr1	27098986	27099128	+
ARID1A	GRCh37/hg19	chr1	27099298	27099483	+
ARID1A	GRCh37/hg19	chr1	27099832	27099992	+
ARID1A	GRCh37/hg19	chr1	27100066	27100213	+
ARID1A	GRCh37/hg19	chr1	27100288	27100394	+
ARID1A	GRCh37/hg19	chr1	27100815	27101716	+
ARID1A	GRCh37/hg19	chr1	27102063	27102203	+
ARID1A	GRCh37/hg19	chr1	27105509	27107252	+
ATRX	GRCh37/hg19	chrX	76763824	76764112	-
ATRX	GRCh37/hg19	chrX	76776261	76776399	-
ATRX	GRCh37/hg19	chrX	76776876	76776981	-
ATRX	GRCh37/hg19	chrX	76777736	76777871	-
ATRX	GRCh37/hg19	chrX	76778725	76778884	-
ATRX	GRCh37/hg19	chrX	76812917	76813121	-
ATRX	GRCh37/hg19	chrX	76814135	76814322	-
ATRX	GRCh37/hg19	chrX	76829710	76829828	-
ATRX	GRCh37/hg19	chrX	76845299	76845415	-
ATRX	GRCh37/hg19	chrX	76849161	76849324	-
ATRX	GRCh37/hg19	chrX	76854875	76855054	-
ATRX	GRCh37/hg19	chrX	76855196	76855294	-
ATRX	GRCh37/hg19	chrX	76855898	76856038	-
ATRX	GRCh37/hg19	chrX	76872076	76872203	-
ATRX	GRCh37/hg19	chrX	76874269	76874454	-
ATRX	GRCh37/hg19	chrX	76875858	76876005	-
ATRX	GRCh37/hg19	chrX	76888690	76888877	-
ATRX	GRCh37/hg19	chrX	76889049	76889205	-
ATRX	GRCh37/hg19	chrX	76890080	76890199	-
ATRX	GRCh37/hg19	chrX	76891401	76891552	-
ATRX	GRCh37/hg19	chrX	76907599	76907848	-
ATRX	GRCh37/hg19	chrX	76909583	76909695	-
ATRX	GRCh37/hg19	chrX	76912045	76912148	-
ATRX	GRCh37/hg19	chrX	76918866	76919052	-
ATRX	GRCh37/hg19	chrX	76920129	76920272	-
ATRX	GRCh37/hg19	chrX	76931716	76931798	-
ATRX	GRCh37/hg19	chrX	76937007	76940090	-
ATRX	GRCh37/hg19	chrX	76940426	76940503	-
ATRX	GRCh37/hg19	chrX	76944306	76944425	-
ATRX	GRCh37/hg19	chrX	76949308	76949431	-
ATRX	GRCh37/hg19	chrX	76952060	76952197	-
ATRX	GRCh37/hg19	chrX	76953066	76953128	-

GENE-EXON	Reference	Chromosome	CHR_Start	CHR_End	STRAND
ATRX	GRCh37/hg19	chrX	76954057	76954122	-
ATRX	GRCh37/hg19	chrX	76972603	76972725	-
ATRX	GRCh37/hg19	chrX	77041463	77041492	-
BAP1	GRCh37/hg19	chr3	52436299	52436442	-
BAP1	GRCh37/hg19	chr3	52436613	52436695	-
BAP1	GRCh37/hg19	chr3	52436790	52436892	-
BAP1	GRCh37/hg19	chr3	52437149	52437319	-
BAP1	GRCh37/hg19	chr3	52437427	52437915	-
BAP1	GRCh37/hg19	chr3	52438464	52438607	-
BAP1	GRCh37/hg19	chr3	52439121	52439315	-
BAP1	GRCh37/hg19	chr3	52439776	52439933	-
BAP1	GRCh37/hg19	chr3	52440264	52440397	-
BAP1	GRCh37/hg19	chr3	52440840	52440928	-
BAP1	GRCh37/hg19	chr3	52441185	52441337	-
BAP1	GRCh37/hg19	chr3	52441410	52441481	-
BAP1	GRCh37/hg19	chr3	52441969	52442098	-
BAP1	GRCh37/hg19	chr3	52442485	52442627	-
BAP1	GRCh37/hg19	chr3	52443565	52443629	-
BAP1	GRCh37/hg19	chr3	52443725	52443764	-
BAP1	GRCh37/hg19	chr3	52443853	52443899	-
BAX	GRCh37/hg19	chr19	49458181	49458224	+
BAX	GRCh37/hg19	chr19	49458800	49458861	+
BAX	GRCh37/hg19	chr19	49458939	49459095	+
BAX	GRCh37/hg19	chr19	49459450	49459595	+
BAX	GRCh37/hg19	chr19	49464062	49464359	+
BAX	GRCh37/hg19	chr19	49464784	49464898	+
BLM	GRCh37/hg19	chr15	91290618	91290725	+
BLM	GRCh37/hg19	chr15	91292592	91293302	+
BLM	GRCh37/hg19	chr15	91295012	91295181	+
BLM	GRCh37/hg19	chr15	91298036	91298173	+
BLM	GRCh37/hg19	chr15	91303372	91303514	+
BLM	GRCh37/hg19	chr15	91303819	91304490	+
BLM	GRCh37/hg19	chr15	91306191	91306392	+
BLM	GRCh37/hg19	chr15	91308521	91308649	+
BLM	GRCh37/hg19	chr15	91310135	91310258	+
BLM	GRCh37/hg19	chr15	91312358	91312466	+
BLM	GRCh37/hg19	chr15	91312663	91312821	+
BLM	GRCh37/hg19	chr15	91326047	91326163	+
BLM	GRCh37/hg19	chr15	91328146	91328316	+
BLM	GRCh37/hg19	chr15	91333874	91334079	+
BLM	GRCh37/hg19	chr15	91337392	91337592	+
BLM	GRCh37/hg19	chr15	91341415	91341572	+
BLM	GRCh37/hg19	chr15	91346746	91346955	+
BLM	GRCh37/hg19	chr15	91347392	91347594	+
BLM	GRCh37/hg19	chr15	91352362	91352494	+
BLM	GRCh37/hg19	chr15	91354430	91354641	+
BLM	GRCh37/hg19	chr15	91358327	91358514	+
CDK4	GRCh37/hg19	chr12	58142303	58142405	-
CDK4	GRCh37/hg19	chr12	58142960	58143105	-
CDK4	GRCh37/hg19	chr12	58143232	58143292	-
CDK4	GRCh37/hg19	chr12	58144434	58144553	-
CDK4	GRCh37/hg19	chr12	58144701	58144878	-
CDK4	GRCh37/hg19	chr12	58144985	58145130	-
CDK4	GRCh37/hg19	chr12	58145278	58145505	-
DAXX	GRCh37/hg19	chr6	33286515	33286584	-
DAXX	GRCh37/hg19	chr6	33286769	33287001	-

GENE-EXON	Reference	Chromosome	CHR_Start	CHR_End	STRAND
DAXX	GRCh37/hg19	chr6	33287152	33287636	-
DAXX	GRCh37/hg19	chr6	33287783	33288006	-
DAXX	GRCh37/hg19	chr6	33288152	33288373	-
DAXX	GRCh37/hg19	chr6	33288508	33289349	-
DAXX	GRCh37/hg19	chr6	33289491	33289707	-
DAXX	GRCh37/hg19	chr6	33290634	33290696	-
FANCM	GRCh37/hg19	chr14	45605230	45605747	+
FANCM	GRCh37/hg19	chr14	45606267	45606449	+
FANCM	GRCh37/hg19	chr14	45609830	45609917	+
FANCM	GRCh37/hg19	chr14	45618035	45618203	+
FANCM	GRCh37/hg19	chr14	45620595	45620736	+
FANCM	GRCh37/hg19	chr14	45623118	45623260	+
FANCM	GRCh37/hg19	chr14	45623895	45624030	+
FANCM	GRCh37/hg19	chr14	45624571	45624667	+
FANCM	GRCh37/hg19	chr14	45628294	45628488	+
FANCM	GRCh37/hg19	chr14	45633557	45633773	+
FANCM	GRCh37/hg19	chr14	45636148	45636371	+
FANCM	GRCh37/hg19	chr14	45639787	45639954	+
FANCM	GRCh37/hg19	chr14	45642253	45642418	+
FANCM	GRCh37/hg19	chr14	45644269	45646184	+
FANCM	GRCh37/hg19	chr14	45650628	45650732	+
FANCM	GRCh37/hg19	chr14	45650835	45650913	+
FANCM	GRCh37/hg19	chr14	45652972	45653110	+
FANCM	GRCh37/hg19	chr14	45654415	45654581	+
FANCM	GRCh37/hg19	chr14	45656979	45657095	+
FANCM	GRCh37/hg19	chr14	45658000	45658570	+
FANCM	GRCh37/hg19	chr14	45665370	45665755	+
FANCM	GRCh37/hg19	chr14	45667842	45668143	+
FANCM	GRCh37/hg19	chr14	45669068	45669216	+
FGFR4	GRCh37/hg19	chr5	176516599	176516699	+
FGFR4	GRCh37/hg19	chr5	176517386	176517659	+
FGFR4	GRCh37/hg19	chr5	176517741	176517831	+
FGFR4	GRCh37/hg19	chr5	176517934	176518110	+
FGFR4	GRCh37/hg19	chr5	176518681	176518814	+
FGFR4	GRCh37/hg19	chr5	176519317	176519517	+
FGFR4	GRCh37/hg19	chr5	176519642	176519790	+
FGFR4	GRCh37/hg19	chr5	176520134	176520337	+
FGFR4	GRCh37/hg19	chr5	176520328	176520557	+
FGFR4	GRCh37/hg19	chr5	176520650	176520781	+
FGFR4	GRCh37/hg19	chr5	176522326	176522446	+
FGFR4	GRCh37/hg19	chr5	176522529	176522729	+
FGFR4	GRCh37/hg19	chr5	176523053	176523185	+
FGFR4	GRCh37/hg19	chr5	176523283	176523363	+
FGFR4	GRCh37/hg19	chr5	176523600	176523747	+
FGFR4	GRCh37/hg19	chr5	176524288	176524403	+
FGFR4	GRCh37/hg19	chr5	176524523	176524682	+
FHIT	GRCh37/hg19	chr3	59737947	59738052	-
FHIT	GRCh37/hg19	chr3	59908067	59908145	-
FHIT	GRCh37/hg19	chr3	59997092	59997131	-
FHIT	GRCh37/hg19	chr3	59999728	59999883	-
FHIT	GRCh37/hg19	chr3	60522588	60522700	-
FLT1	GRCh37/hg19	chr13	28877299	28877510	-
FLT1	GRCh37/hg19	chr13	28880810	28880914	-
FLT1	GRCh37/hg19	chr13	28882975	28883069	-
FLT1	GRCh37/hg19	chr13	28885722	28885874	-
FLT1	GRCh37/hg19	chr13	28886125	28886240	-

GENE-EXON	Reference	Chromosome	CHR_Start	CHR_End	STRAND
FLT1	GRCh37/hg19	chr13	28891630	28891739	-
FLT1	GRCh37/hg19	chr13	28893555	28893676	-
FLT1	GRCh37/hg19	chr13	28895595	28895727	-
FLT1	GRCh37/hg19	chr13	28896394	28896501	-
FLT1	GRCh37/hg19	chr13	28896922	28897088	-
FLT1	GRCh37/hg19	chr13	28901594	28901692	-
FLT1	GRCh37/hg19	chr13	28903747	28903870	-
FLT1	GRCh37/hg19	chr13	28908157	28908271	-
FLT1	GRCh37/hg19	chr13	28913300	28913442	-
FLT1	GRCh37/hg19	chr13	28919577	28919693	-
FLT1	GRCh37/hg19	chr13	28931686	28931827	-
FLT1	GRCh37/hg19	chr13	28942710	28942805	-
FLT1	GRCh37/hg19	chr13	28959017	28959173	-
FLT1	GRCh37/hg19	chr13	28963833	28964246	-
FLT1	GRCh37/hg19	chr13	28971092	28971210	-
FLT1	GRCh37/hg19	chr13	28973176	28973260	-
FLT1	GRCh37/hg19	chr13	28979912	28980036	-
FLT1	GRCh37/hg19	chr13	29001291	29001460	-
FLT1	GRCh37/hg19	chr13	29001884	29002063	-
FLT1	GRCh37/hg19	chr13	29004182	29004309	-
FLT1	GRCh37/hg19	chr13	29005268	29005452	-
FLT1	GRCh37/hg19	chr13	29007951	29008097	-
FLT1	GRCh37/hg19	chr13	29008190	29008362	-
FLT1	GRCh37/hg19	chr13	29012353	29012487	-
FLT1	GRCh37/hg19	chr13	29041035	29041271	-
FLT1	GRCh37/hg19	chr13	29041653	29041759	-
FLT1	GRCh37/hg19	chr13	29068912	29068985	-
FLT4	GRCh37/hg19	chr5	180030187	180030395	-
FLT4	GRCh37/hg19	chr5	180035276	180035289	-
FLT4	GRCh37/hg19	chr5	180035963	180036058	-
FLT4	GRCh37/hg19	chr5	180036900	180037030	-
FLT4	GRCh37/hg19	chr5	180038326	180038484	-
FLT4	GRCh37/hg19	chr5	180039501	180039616	-
FLT4	GRCh37/hg19	chr5	180040006	180040115	-
FLT4	GRCh37/hg19	chr5	180041063	180041184	-
FLT4	GRCh37/hg19	chr5	180043362	180043494	-
FLT4	GRCh37/hg19	chr5	180043895	180043999	-
FLT4	GRCh37/hg19	chr5	180045765	180045925	-
FLT4	GRCh37/hg19	chr5	180046016	180046114	-
FLT4	GRCh37/hg19	chr5	180046248	180046371	-
FLT4	GRCh37/hg19	chr5	180046660	180046774	-
FLT4	GRCh37/hg19	chr5	180047168	180047313	-
FLT4	GRCh37/hg19	chr5	180047604	180047720	-
FLT4	GRCh37/hg19	chr5	180047871	180048012	-
FLT4	GRCh37/hg19	chr5	180048101	180048257	-
FLT4	GRCh37/hg19	chr5	180048537	180048909	-
FLT4	GRCh37/hg19	chr5	180049726	180049844	-
FLT4	GRCh37/hg19	chr5	180050930	180051066	-
FLT4	GRCh37/hg19	chr5	180052864	180053036	-
FLT4	GRCh37/hg19	chr5	180053106	180053270	-
FLT4	GRCh37/hg19	chr5	180055877	180056004	-
FLT4	GRCh37/hg19	chr5	180056254	180056432	-
FLT4	GRCh37/hg19	chr5	180056691	180056840	-
FLT4	GRCh37/hg19	chr5	180056938	180057110	-
FLT4	GRCh37/hg19	chr5	180057220	180057342	-
FLT4	GRCh37/hg19	chr5	180057550	180057804	-

GENE-EXON	Reference	Chromosome	CHR_Start	CHR_End	STRAND
FLT4	GRCh37/hg19	chr5	180058677	180058783	-
FLT4	GRCh37/hg19	chr5	180076483	180076550	-
FOXA1	GRCh37/hg19	chr14	38060565	38061921	-
FOXA1	GRCh37/hg19	chr14	38064101	38064182	-
GATA3	GRCh37/hg19	chr10	8097614	8097864	+
GATA3	GRCh37/hg19	chr10	8100263	8100809	+
GATA3	GRCh37/hg19	chr10	8105951	8106106	+
GATA3	GRCh37/hg19	chr10	8111431	8111566	+
GATA3	GRCh37/hg19	chr10	8115697	8115991	+
GRM3	GRCh37/hg19	chr7	86394457	86394934	+
GRM3	GRCh37/hg19	chr7	86415572	86416437	+
GRM3	GRCh37/hg19	chr7	86468150	86469226	+
GRM3	GRCh37/hg19	chr7	86479681	86479865	+
GRM3	GRCh37/hg19	chr7	86493593	86493676	+
IGF1R	GRCh37/hg19	chr15	99192806	99192909	+
IGF1R	GRCh37/hg19	chr15	99250786	99251341	+
IGF1R	GRCh37/hg19	chr15	99434549	99434871	+
IGF1R	GRCh37/hg19	chr15	99439981	99440139	+
IGF1R	GRCh37/hg19	chr15	99442701	99442855	+
IGF1R	GRCh37/hg19	chr15	99451909	99452133	+
IGF1R	GRCh37/hg19	chr15	99454539	99454675	+
IGF1R	GRCh37/hg19	chr15	99456268	99456516	+
IGF1R	GRCh37/hg19	chr15	99459188	99459365	+
IGF1R	GRCh37/hg19	chr15	99459896	99460110	+
IGF1R	GRCh37/hg19	chr15	99465372	99465665	+
IGF1R	GRCh37/hg19	chr15	99467100	99467246	+
IGF1R	GRCh37/hg19	chr15	99467749	99467918	+
IGF1R	GRCh37/hg19	chr15	99472782	99472894	+
IGF1R	GRCh37/hg19	chr15	99473459	99473539	+
IGF1R	GRCh37/hg19	chr15	99478048	99478287	+
IGF1R	GRCh37/hg19	chr15	99478540	99478660	+
IGF1R	GRCh37/hg19	chr15	99482425	99482594	+
IGF1R	GRCh37/hg19	chr15	99486147	99486286	+
IGF1R	GRCh37/hg19	chr15	99491798	99491942	+
IGF1R	GRCh37/hg19	chr15	99500285	99500676	+
IGF2R	GRCh37/hg19	chr6	160390274	160390432	+
IGF2R	GRCh37/hg19	chr6	160412211	160412360	+
IGF2R	GRCh37/hg19	chr6	160430037	160430171	+
IGF2R	GRCh37/hg19	chr6	160431714	160431822	+
IGF2R	GRCh37/hg19	chr6	160445599	160445741	+
IGF2R	GRCh37/hg19	chr6	160448212	160448351	+
IGF2R	GRCh37/hg19	chr6	160450577	160450692	+
IGF2R	GRCh37/hg19	chr6	160453578	160453750	+
IGF2R	GRCh37/hg19	chr6	160453969	160454144	+
IGF2R	GRCh37/hg19	chr6	160455446	160455559	+
IGF2R	GRCh37/hg19	chr6	160461587	160461761	+
IGF2R	GRCh37/hg19	chr6	160464175	160464325	+
IGF2R	GRCh37/hg19	chr6	160465541	160465694	+
IGF2R	GRCh37/hg19	chr6	160466772	160466919	+
IGF2R	GRCh37/hg19	chr6	160467525	160467682	+
IGF2R	GRCh37/hg19	chr6	160468186	160468373	+
IGF2R	GRCh37/hg19	chr6	160468819	160468944	+
IGF2R	GRCh37/hg19	chr6	160469402	160469580	+
IGF2R	GRCh37/hg19	chr6	160471500	160471689	+
IGF2R	GRCh37/hg19	chr6	160477451	160477562	+
IGF2R	GRCh37/hg19	chr6	160479050	160479161	+

GENE-EXON	Reference	Chromosome	CHR_Start	CHR_End	STRAND
IGF2R	GRCh37/hg19	chr6	160479933	160480135	+
IGF2R	GRCh37/hg19	chr6	160481574	160481754	+
IGF2R	GRCh37/hg19	chr6	160482530	160482683	+
IGF2R	GRCh37/hg19	chr6	160482780	160482965	+
IGF2R	GRCh37/hg19	chr6	160483559	160483656	+
IGF2R	GRCh37/hg19	chr6	160484442	160484667	+
IGF2R	GRCh37/hg19	chr6	160485428	160485568	+
IGF2R	GRCh37/hg19	chr6	160485831	160485938	+
IGF2R	GRCh37/hg19	chr6	160489276	160489422	+
IGF2R	GRCh37/hg19	chr6	160490895	160491095	+
IGF2R	GRCh37/hg19	chr6	160492937	160493073	+
IGF2R	GRCh37/hg19	chr6	160493792	160493921	+
IGF2R	GRCh37/hg19	chr6	160494240	160494506	+
IGF2R	GRCh37/hg19	chr6	160494784	160495012	+
IGF2R	GRCh37/hg19	chr6	160496874	160497033	+
IGF2R	GRCh37/hg19	chr6	160499228	160499399	+
IGF2R	GRCh37/hg19	chr6	160500607	160500824	+
IGF2R	GRCh37/hg19	chr6	160501156	160501312	+
IGF2R	GRCh37/hg19	chr6	160504977	160505221	+
IGF2R	GRCh37/hg19	chr6	160506022	160506168	+
IGF2R	GRCh37/hg19	chr6	160509060	160509184	+
IGF2R	GRCh37/hg19	chr6	160510134	160510290	+
IGF2R	GRCh37/hg19	chr6	160510943	160511140	+
IGF2R	GRCh37/hg19	chr6	160517466	160517662	+
IGF2R	GRCh37/hg19	chr6	160523546	160523708	+
IGF2R	GRCh37/hg19	chr6	160524773	160524852	+
IGF2R	GRCh37/hg19	chr6	160525701	160526121	+
KDM5C	GRCh37/hg19	chrX	53221921	53222024	-
KDM5C	GRCh37/hg19	chrX	53222144	53222519	-
KDM5C	GRCh37/hg19	chrX	53222614	53222823	-
KDM5C	GRCh37/hg19	chrX	53222950	53223038	-
KDM5C	GRCh37/hg19	chrX	53223316	53223925	-
KDM5C	GRCh37/hg19	chrX	53224108	53224255	-
KDM5C	GRCh37/hg19	chrX	53224408	53224597	-
KDM5C	GRCh37/hg19	chrX	53225093	53225241	-
KDM5C	GRCh37/hg19	chrX	53225863	53226231	-
KDM5C	GRCh37/hg19	chrX	53226948	53227063	-
KDM5C	GRCh37/hg19	chrX	53227667	53227824	-
KDM5C	GRCh37/hg19	chrX	53227941	53228075	-
KDM5C	GRCh37/hg19	chrX	53228154	53228345	-
KDM5C	GRCh37/hg19	chrX	53230727	53230931	-
KDM5C	GRCh37/hg19	chrX	53231031	53231160	-
KDM5C	GRCh37/hg19	chrX	53239591	53239763	-
KDM5C	GRCh37/hg19	chrX	53239853	53240044	-
KDM5C	GRCh37/hg19	chrX	53240674	53240842	-
KDM5C	GRCh37/hg19	chrX	53240964	53241093	-
KDM5C	GRCh37/hg19	chrX	53243866	53244034	-
KDM5C	GRCh37/hg19	chrX	53244972	53245163	-
KDM5C	GRCh37/hg19	chrX	53245251	53245384	-
KDM5C	GRCh37/hg19	chrX	53246320	53246464	-
KDM5C	GRCh37/hg19	chrX	53246973	53247153	-
KDM5C	GRCh37/hg19	chrX	53247453	53247585	-
KDM5C	GRCh37/hg19	chrX	53250016	53250103	-
KDM5C	GRCh37/hg19	chrX	53253917	53254076	-
KMT2C	GRCh37/hg19	chr7	151833912	151834014	-
KMT2C	GRCh37/hg19	chr7	151835876	151835994	-

GENE-EXON	Reference	Chromosome	CHR_Start	CHR_End	STRAND
KMT2C	GRCh37/hg19	chr7	151836266	151836349	-
KMT2C	GRCh37/hg19	chr7	151836755	151836881	-
KMT2C	GRCh37/hg19	chr7	151841793	151841971	-
KMT2C	GRCh37/hg19	chr7	151842233	151842385	-
KMT2C	GRCh37/hg19	chr7	151843679	151843825	-
KMT2C	GRCh37/hg19	chr7	151845113	151846242	-
KMT2C	GRCh37/hg19	chr7	151847980	151848097	-
KMT2C	GRCh37/hg19	chr7	151848522	151848671	-
KMT2C	GRCh37/hg19	chr7	151849785	151850044	-
KMT2C	GRCh37/hg19	chr7	151851090	151851236	-
KMT2C	GRCh37/hg19	chr7	151851347	151851535	-
KMT2C	GRCh37/hg19	chr7	151852990	151853147	-
KMT2C	GRCh37/hg19	chr7	151853285	151853436	-
KMT2C	GRCh37/hg19	chr7	151855943	151856162	-
KMT2C	GRCh37/hg19	chr7	151859197	151860916	-
KMT2C	GRCh37/hg19	chr7	151864226	151864468	-
KMT2C	GRCh37/hg19	chr7	151866266	151866339	-
KMT2C	GRCh37/hg19	chr7	151868344	151868432	-
KMT2C	GRCh37/hg19	chr7	151871211	151871332	-
KMT2C	GRCh37/hg19	chr7	151873271	151875100	-
KMT2C	GRCh37/hg19	chr7	151876914	151877216	-
KMT2C	GRCh37/hg19	chr7	151877791	151879684	-
KMT2C	GRCh37/hg19	chr7	151880054	151880246	-
KMT2C	GRCh37/hg19	chr7	151882638	151882721	-
KMT2C	GRCh37/hg19	chr7	151884342	151884566	-
KMT2C	GRCh37/hg19	chr7	151884795	151884937	-
KMT2C	GRCh37/hg19	chr7	151891089	151891218	-
KMT2C	GRCh37/hg19	chr7	151891309	151891351	-
KMT2C	GRCh37/hg19	chr7	151891520	151891658	-
KMT2C	GRCh37/hg19	chr7	151892987	151893101	-
KMT2C	GRCh37/hg19	chr7	151896359	151896549	-
KMT2C	GRCh37/hg19	chr7	151900014	151900154	-
KMT2C	GRCh37/hg19	chr7	151902186	151902315	-
KMT2C	GRCh37/hg19	chr7	151904380	151904518	-
KMT2C	GRCh37/hg19	chr7	151917603	151917825	-
KMT2C	GRCh37/hg19	chr7	151919081	151919156	-
KMT2C	GRCh37/hg19	chr7	151919653	151919772	-
KMT2C	GRCh37/hg19	chr7	151921095	151921269	-
KMT2C	GRCh37/hg19	chr7	151921515	151921706	-
KMT2C	GRCh37/hg19	chr7	151927003	151927117	-
KMT2C	GRCh37/hg19	chr7	151927300	151927411	-
KMT2C	GRCh37/hg19	chr7	151932897	151933023	-
KMT2C	GRCh37/hg19	chr7	151935787	151935916	-
KMT2C	GRCh37/hg19	chr7	151944982	151945710	-
KMT2C	GRCh37/hg19	chr7	151946956	151947043	-
KMT2C	GRCh37/hg19	chr7	151947933	151948056	-
KMT2C	GRCh37/hg19	chr7	151949019	151949180	-
KMT2C	GRCh37/hg19	chr7	151949626	151949805	-
KMT2C	GRCh37/hg19	chr7	151960096	151960220	-
KMT2C	GRCh37/hg19	chr7	151962118	151962299	-
KMT2C	GRCh37/hg19	chr7	151970785	151970957	-
KMT2C	GRCh37/hg19	chr7	152007046	152007165	-
KMT2C	GRCh37/hg19	chr7	152008878	152009036	-
KMT2C	GRCh37/hg19	chr7	152012218	152012428	-
KMT2C	GRCh37/hg19	chr7	152027681	152027829	-
KMT2C	GRCh37/hg19	chr7	152055667	152055765	-

GENE-EXON	Reference	Chromosome	CHR_Start	CHR_End	STRAND
KMT2C	GRCh37/hg19	chr7	152132706	152132876	-
MED12	GRCh37/hg19	chrX	70338600	70338708	+
MED12	GRCh37/hg19	chrX	70339218	70339332	+
MED12	GRCh37/hg19	chrX	70339531	70339732	+
MED12	GRCh37/hg19	chrX	70339859	70340025	+
MED12	GRCh37/hg19	chrX	70340816	70341007	+
MED12	GRCh37/hg19	chrX	70341172	70341292	+
MED12	GRCh37/hg19	chrX	70341407	70341671	+
MED12	GRCh37/hg19	chrX	70342045	70342201	+
MED12	GRCh37/hg19	chrX	70342353	70342462	+
MED12	GRCh37/hg19	chrX	70342583	70342729	+
MED12	GRCh37/hg19	chrX	70342940	70343081	+
MED12	GRCh37/hg19	chrX	70343439	70343575	+
MED12	GRCh37/hg19	chrX	70344004	70344243	+
MED12	GRCh37/hg19	chrX	70344609	70344699	+
MED12	GRCh37/hg19	chrX	70344821	70345001	+
MED12	GRCh37/hg19	chrX	70345196	70345350	+
MED12	GRCh37/hg19	chrX	70345508	70345568	+
MED12	GRCh37/hg19	chrX	70345881	70346009	+
MED12	GRCh37/hg19	chrX	70346186	70346339	+
MED12	GRCh37/hg19	chrX	70346814	70346987	+
MED12	GRCh37/hg19	chrX	70347181	70347322	+
MED12	GRCh37/hg19	chrX	70347738	70347975	+
MED12	GRCh37/hg19	chrX	70348141	70348295	+
MED12	GRCh37/hg19	chrX	70348443	70348573	+
MED12	GRCh37/hg19	chrX	70348959	70349070	+
MED12	GRCh37/hg19	chrX	70349161	70349284	+
MED12	GRCh37/hg19	chrX	70349525	70349710	+
MED12	GRCh37/hg19	chrX	70349880	70350069	+
MED12	GRCh37/hg19	chrX	70351395	70351476	+
MED12	GRCh37/hg19	chrX	70351918	70352061	+
MED12	GRCh37/hg19	chrX	70352222	70352393	+
MED12	GRCh37/hg19	chrX	70352690	70352811	+
MED12	GRCh37/hg19	chrX	70352968	70353067	+
MED12	GRCh37/hg19	chrX	70354202	70354321	+
MED12	GRCh37/hg19	chrX	70354558	70354703	+
MED12	GRCh37/hg19	chrX	70354937	70355108	+
MED12	GRCh37/hg19	chrX	70356126	70356510	+
MED12	GRCh37/hg19	chrX	70356724	70356884	+
MED12	GRCh37/hg19	chrX	70357032	70357238	+
MED12	GRCh37/hg19	chrX	70357403	70357490	+
MED12	GRCh37/hg19	chrX	70357571	70357798	+
MED12	GRCh37/hg19	chrX	70360480	70360712	+
MED12	GRCh37/hg19	chrX	70361075	70361225	+
MED12	GRCh37/hg19	chrX	70361728	70361819	+
MED12	GRCh37/hg19	chrX	70362020	70362073	+
MEN1	GRCh37/hg19	chr11	64571801	64572293	-
MEN1	GRCh37/hg19	chr11	64572501	64572675	-
MEN1	GRCh37/hg19	chr11	64573102	64573247	-
MEN1	GRCh37/hg19	chr11	64573699	64573845	-
MEN1	GRCh37/hg19	chr11	64574478	64574575	-
MEN1	GRCh37/hg19	chr11	64574646	64574696	-
MEN1	GRCh37/hg19	chr11	64575019	64575157	-
MEN1	GRCh37/hg19	chr11	64575358	64575576	-
MEN1	GRCh37/hg19	chr11	64577117	64577586	-
MSH2	GRCh37/hg19	chr2	47630326	47630546	+

GENE-EXON	Reference	Chromosome	CHR_Start	CHR_End	STRAND
MSH2	GRCh37/hg19	chr2	47635535	47635699	+
MSH2	GRCh37/hg19	chr2	47637228	47637516	+
MSH2	GRCh37/hg19	chr2	47639548	47639704	+
MSH2	GRCh37/hg19	chr2	47641403	47641562	+
MSH2	GRCh37/hg19	chr2	47643430	47643573	+
MSH2	GRCh37/hg19	chr2	47656876	47657085	+
MSH2	GRCh37/hg19	chr2	47672682	47672801	+
MSH2	GRCh37/hg19	chr2	47690165	47690298	+
MSH2	GRCh37/hg19	chr2	47693792	47693952	+
MSH2	GRCh37/hg19	chr2	47698099	47698206	+
MSH2	GRCh37/hg19	chr2	47702159	47702414	+
MSH2	GRCh37/hg19	chr2	47703501	47703715	+
MSH2	GRCh37/hg19	chr2	47705406	47705663	+
MSH2	GRCh37/hg19	chr2	47707830	47708015	+
MSH2	GRCh37/hg19	chr2	47709913	47710093	+
MSH6	GRCh37/hg19	chr2	48010368	48010637	+
MSH6	GRCh37/hg19	chr2	48018061	48018267	+
MSH6	GRCh37/hg19	chr2	48023028	48023207	+
MSH6	GRCh37/hg19	chr2	48025745	48028299	+
MSH6	GRCh37/hg19	chr2	48030554	48030829	+
MSH6	GRCh37/hg19	chr2	48032044	48032171	+
MSH6	GRCh37/hg19	chr2	48032752	48032851	+
MSH6	GRCh37/hg19	chr2	48033338	48033502	+
MSH6	GRCh37/hg19	chr2	48033586	48033795	+
MSH6	GRCh37/hg19	chr2	48033913	48034004	+
MTOR	GRCh37/hg19	chr1	11167537	11167562	-
MTOR	GRCh37/hg19	chr1	11168233	11168348	-
MTOR	GRCh37/hg19	chr1	11169342	11169432	-
MTOR	GRCh37/hg19	chr1	11169701	11169791	-
MTOR	GRCh37/hg19	chr1	11172904	11172979	-
MTOR	GRCh37/hg19	chr1	11174370	11174515	-
MTOR	GRCh37/hg19	chr1	11174865	11174949	-
MTOR	GRCh37/hg19	chr1	11175448	11175530	-
MTOR	GRCh37/hg19	chr1	11177056	11177148	-
MTOR	GRCh37/hg19	chr1	11181298	11181430	-
MTOR	GRCh37/hg19	chr1	11182031	11182188	-
MTOR	GRCh37/hg19	chr1	11184550	11184695	-
MTOR	GRCh37/hg19	chr1	11186674	11186858	-
MTOR	GRCh37/hg19	chr1	11187062	11187206	-
MTOR	GRCh37/hg19	chr1	11187676	11187868	-
MTOR	GRCh37/hg19	chr1	11188056	11188188	-
MTOR	GRCh37/hg19	chr1	11188506	11188614	-
MTOR	GRCh37/hg19	chr1	11188907	11189013	-
MTOR	GRCh37/hg19	chr1	11189790	11189900	-
MTOR	GRCh37/hg19	chr1	11190581	11190839	-
MTOR	GRCh37/hg19	chr1	11193132	11193259	-
MTOR	GRCh37/hg19	chr1	11194403	11194528	-
MTOR	GRCh37/hg19	chr1	11199356	11199497	-
MTOR	GRCh37/hg19	chr1	11199585	11199720	-
MTOR	GRCh37/hg19	chr1	11204700	11204817	-
MTOR	GRCh37/hg19	chr1	11205020	11205107	-
MTOR	GRCh37/hg19	chr1	11206728	11206853	-
MTOR	GRCh37/hg19	chr1	11210178	11210288	-
MTOR	GRCh37/hg19	chr1	11217204	11217353	-
MTOR	GRCh37/hg19	chr1	11227494	11227579	-
MTOR	GRCh37/hg19	chr1	11259310	11259465	-

GENE-EXON	Reference	Chromosome	CHR_Start	CHR_End	STRAND
MTOR	GRCh37/hg19	chr1	11259593	11259765	-
MTOR	GRCh37/hg19	chr1	11264613	11264765	-
MTOR	GRCh37/hg19	chr1	11269364	11269520	-
MTOR	GRCh37/hg19	chr1	11270866	11270968	-
MTOR	GRCh37/hg19	chr1	11272364	11272536	-
MTOR	GRCh37/hg19	chr1	11272848	11272970	-
MTOR	GRCh37/hg19	chr1	11273451	11273628	-
MTOR	GRCh37/hg19	chr1	11276200	11276296	-
MTOR	GRCh37/hg19	chr1	11288720	11288980	-
MTOR	GRCh37/hg19	chr1	11290977	11291116	-
MTOR	GRCh37/hg19	chr1	11291352	11291496	-
MTOR	GRCh37/hg19	chr1	11292488	11292590	-
MTOR	GRCh37/hg19	chr1	11293450	11293549	-
MTOR	GRCh37/hg19	chr1	11294195	11294327	-
MTOR	GRCh37/hg19	chr1	11297895	11298110	-
MTOR	GRCh37/hg19	chr1	11298454	11298679	-
MTOR	GRCh37/hg19	chr1	11300355	11300609	-
MTOR	GRCh37/hg19	chr1	11301605	11301743	-
MTOR	GRCh37/hg19	chr1	11303166	11303362	-
MTOR	GRCh37/hg19	chr1	11307677	11307795	-
MTOR	GRCh37/hg19	chr1	11307871	11308156	-
MTOR	GRCh37/hg19	chr1	11313891	11314035	-
MTOR	GRCh37/hg19	chr1	11316044	11316254	-
MTOR	GRCh37/hg19	chr1	11316985	11317227	-
MTOR	GRCh37/hg19	chr1	11318537	11318655	-
MTOR	GRCh37/hg19	chr1	11319300	11319471	-
NF1	GRCh37/hg19	chr17	29422323	29422392	+
NF1	GRCh37/hg19	chr17	29482996	29483149	+
NF1	GRCh37/hg19	chr17	29486023	29486116	+
NF1	GRCh37/hg19	chr17	29490199	29490399	+
NF1	GRCh37/hg19	chr17	29496904	29497020	+
NF1	GRCh37/hg19	chr17	29508435	29508512	+
NF1	GRCh37/hg19	chr17	29508723	29508808	+
NF1	GRCh37/hg19	chr17	29509521	29509688	+
NF1	GRCh37/hg19	chr17	29527435	29527618	+
NF1	GRCh37/hg19	chr17	29528050	29528182	+
NF1	GRCh37/hg19	chr17	29528424	29528508	+
NF1	GRCh37/hg19	chr17	29533253	29533394	+
NF1	GRCh37/hg19	chr17	29541464	29541608	+
NF1	GRCh37/hg19	chr17	29546018	29546141	+
NF1	GRCh37/hg19	chr17	29548863	29549013	+
NF1	GRCh37/hg19	chr17	29550457	29550590	+
NF1	GRCh37/hg19	chr17	29552108	29552273	+
NF1	GRCh37/hg19	chr17	29553448	29553707	+
NF1	GRCh37/hg19	chr17	29554231	29554314	+
NF1	GRCh37/hg19	chr17	29554536	29554629	+
NF1	GRCh37/hg19	chr17	29556038	29556488	+
NF1	GRCh37/hg19	chr17	29556848	29556997	+
NF1	GRCh37/hg19	chr17	29557273	29557405	+
NF1	GRCh37/hg19	chr17	29557855	29557948	+
NF1	GRCh37/hg19	chr17	29559086	29559212	+
NF1	GRCh37/hg19	chr17	29559713	29559904	+
NF1	GRCh37/hg19	chr17	29560015	29560236	+
NF1	GRCh37/hg19	chr17	29562624	29562795	+
NF1	GRCh37/hg19	chr17	29562931	29563044	+
NF1	GRCh37/hg19	chr17	29575997	29576142	+

GENE-EXON	Reference	Chromosome	CHR_Start	CHR_End	STRAND
NF1	GRCh37/hg19	chr17	29579951	29580023	+
NF1	GRCh37/hg19	chr17	29585357	29585525	+
NF1	GRCh37/hg19	chr17	29586045	29586152	+
NF1	GRCh37/hg19	chr17	29587382	29587538	+
NF1	GRCh37/hg19	chr17	29588724	29588880	+
NF1	GRCh37/hg19	chr17	29592242	29592362	+
NF1	GRCh37/hg19	chr17	29652833	29653275	+
NF1	GRCh37/hg19	chr17	29654512	29654862	+
NF1	GRCh37/hg19	chr17	29657309	29657521	+
NF1	GRCh37/hg19	chr17	29661851	29662054	+
NF1	GRCh37/hg19	chr17	29663346	29663496	+
NF1	GRCh37/hg19	chr17	29663648	29663937	+
NF1	GRCh37/hg19	chr17	29664381	29664605	+
NF1	GRCh37/hg19	chr17	29664832	29664903	+
NF1	GRCh37/hg19	chr17	29665038	29665162	+
NF1	GRCh37/hg19	chr17	29665717	29665828	+
NF1	GRCh37/hg19	chr17	29667518	29667668	+
NF1	GRCh37/hg19	chr17	29670022	29670158	+
NF1	GRCh37/hg19	chr17	29676133	29676274	+
NF1	GRCh37/hg19	chr17	29677196	29677341	+
NF1	GRCh37/hg19	chr17	29679270	29679437	+
NF1	GRCh37/hg19	chr17	29683473	29683605	+
NF1	GRCh37/hg19	chr17	29683973	29684113	+
NF1	GRCh37/hg19	chr17	29684282	29684392	+
NF1	GRCh37/hg19	chr17	29685493	29685645	+
NF1	GRCh37/hg19	chr17	29685982	29686038	+
NF1	GRCh37/hg19	chr17	29687500	29687726	+
NF1	GRCh37/hg19	chr17	29701026	29701178	+
PBRM1	GRCh37/hg19	chr3	52582074	52582256	-
PBRM1	GRCh37/hg19	chr3	52584432	52584658	-
PBRM1	GRCh37/hg19	chr3	52584758	52584838	-
PBRM1	GRCh37/hg19	chr3	52588735	52588900	-
PBRM1	GRCh37/hg19	chr3	52595778	52595989	-
PBRM1	GRCh37/hg19	chr3	52597375	52597514	-
PBRM1	GRCh37/hg19	chr3	52598061	52598254	-
PBRM1	GRCh37/hg19	chr3	52610552	52610719	-
PBRM1	GRCh37/hg19	chr3	52613065	52613220	-
PBRM1	GRCh37/hg19	chr3	52620436	52620709	-
PBRM1	GRCh37/hg19	chr3	52621364	52621456	-
PBRM1	GRCh37/hg19	chr3	52623081	52623276	-
PBRM1	GRCh37/hg19	chr3	52637532	52637753	-
PBRM1	GRCh37/hg19	chr3	52643324	52643976	-
PBRM1	GRCh37/hg19	chr3	52649362	52649477	-
PBRM1	GRCh37/hg19	chr3	52651273	52651559	-
PBRM1	GRCh37/hg19	chr3	52661284	52661391	-
PBRM1	GRCh37/hg19	chr3	52662905	52663056	-
PBRM1	GRCh37/hg19	chr3	52668613	52668836	-
PBRM1	GRCh37/hg19	chr3	52675965	52676066	-
PBRM1	GRCh37/hg19	chr3	52677259	52677364	-
PBRM1	GRCh37/hg19	chr3	52678715	52678810	-
PBRM1	GRCh37/hg19	chr3	52682355	52682463	-
PBRM1	GRCh37/hg19	chr3	52685753	52685831	-
PBRM1	GRCh37/hg19	chr3	52692210	52692336	-
PBRM1	GRCh37/hg19	chr3	52696144	52696297	-
PBRM1	GRCh37/hg19	chr3	52702509	52702666	-
PBRM1	GRCh37/hg19	chr3	52712511	52712618	-

GENE-EXON	Reference	Chromosome	CHR_Start	CHR_End	STRAND
PBRM1	GRCh37/hg19	chr3	52713585	52713732	-
PDGFRB	GRCh37/hg19	chr5	149495321	149495514	-
PDGFRB	GRCh37/hg19	chr5	149497176	149497418	-
PDGFRB	GRCh37/hg19	chr5	149498305	149498420	-
PDGFRB	GRCh37/hg19	chr5	149499025	149499134	-
PDGFRB	GRCh37/hg19	chr5	149499570	149499691	-
PDGFRB	GRCh37/hg19	chr5	149500446	149500578	-
PDGFRB	GRCh37/hg19	chr5	149500762	149500890	-
PDGFRB	GRCh37/hg19	chr5	149501438	149501608	-
PDGFRB	GRCh37/hg19	chr5	149502600	149502769	-
PDGFRB	GRCh37/hg19	chr5	149503808	149503928	-
PDGFRB	GRCh37/hg19	chr5	149504285	149504399	-
PDGFRB	GRCh37/hg19	chr5	149505003	149505145	-
PDGFRB	GRCh37/hg19	chr5	149506078	149506182	-
PDGFRB	GRCh37/hg19	chr5	149509315	149509536	-
PDGFRB	GRCh37/hg19	chr5	149510097	149510230	-
PDGFRB	GRCh37/hg19	chr5	149511537	149511662	-
PDGFRB	GRCh37/hg19	chr5	149512308	149512510	-
PDGFRB	GRCh37/hg19	chr5	149513144	149513328	-
PDGFRB	GRCh37/hg19	chr5	149513439	149513576	-
PDGFRB	GRCh37/hg19	chr5	149514308	149514584	-
PDGFRB	GRCh37/hg19	chr5	149515113	149515446	-
PDGFRB	GRCh37/hg19	chr5	149516566	149516615	-
PIK3R1	GRCh37/hg19	chr5	67522499	67522842	+
PIK3R1	GRCh37/hg19	chr5	67569213	67569315	+
PIK3R1	GRCh37/hg19	chr5	67569762	67569846	+
PIK3R1	GRCh37/hg19	chr5	67575425	67575566	+
PIK3R1	GRCh37/hg19	chr5	67576351	67576562	+
PIK3R1	GRCh37/hg19	chr5	67576750	67576839	+
PIK3R1	GRCh37/hg19	chr5	67584559	67584584	+
PIK3R1	GRCh37/hg19	chr5	67586552	67586667	+
PIK3R1	GRCh37/hg19	chr5	67588082	67588194	+
PIK3R1	GRCh37/hg19	chr5	67588924	67589032	+
PIK3R1	GRCh37/hg19	chr5	67589126	67589316	+
PIK3R1	GRCh37/hg19	chr5	67589532	67589667	+
PIK3R1	GRCh37/hg19	chr5	67590359	67590511	+
PIK3R1	GRCh37/hg19	chr5	67590971	67591157	+
PIK3R1	GRCh37/hg19	chr5	67591243	67591321	+
PIK3R1	GRCh37/hg19	chr5	67591994	67592174	+
PIK3R1	GRCh37/hg19	chr5	67593235	67593434	+
PMS2	GRCh37/hg19	chr7	6013025	6013178	-
PMS2	GRCh37/hg19	chr7	6017214	6017393	-
PMS2	GRCh37/hg19	chr7	6018222	6018332	-
PMS2	GRCh37/hg19	chr7	6022450	6022627	-
PMS2	GRCh37/hg19	chr7	6026385	6027256	-
PMS2	GRCh37/hg19	chr7	6029426	6029591	-
PMS2	GRCh37/hg19	chr7	6031599	6031693	-
PMS2	GRCh37/hg19	chr7	6035160	6035269	-
PMS2	GRCh37/hg19	chr7	6036952	6037059	-
PMS2	GRCh37/hg19	chr7	6038734	6038911	-
PMS2	GRCh37/hg19	chr7	6042079	6042272	-
PMS2	GRCh37/hg19	chr7	6043316	6043428	-
PMS2	GRCh37/hg19	chr7	6043598	6043694	-
PMS2	GRCh37/hg19	chr7	6045518	6045667	-
PMS2	GRCh37/hg19	chr7	6048623	6048655	-
POLK	GRCh37/hg19	chr5	74842843	74842987	+

GENE-EXON	Reference	Chromosome	CHR_Start	CHR_End	STRAND
POLK	GRCh37/hg19	chr5	74848292	74848421	+
POLK	GRCh37/hg19	chr5	74865160	74865322	+
POLK	GRCh37/hg19	chr5	74869558	74869699	+
POLK	GRCh37/hg19	chr5	74872600	74872763	+
POLK	GRCh37/hg19	chr5	74877029	74877278	+
POLK	GRCh37/hg19	chr5	74879113	74879247	+
POLK	GRCh37/hg19	chr5	74880580	74880756	+
POLK	GRCh37/hg19	chr5	74882846	74882888	+
POLK	GRCh37/hg19	chr5	74886164	74886270	+
POLK	GRCh37/hg19	chr5	74889698	74889879	+
POLK	GRCh37/hg19	chr5	74892042	74893008	+
POLK	GRCh37/hg19	chr5	74893567	74893619	+
POLK	GRCh37/hg19	chr5	74893754	74893848	+
PRKDC	GRCh37/hg19	chr8	48686729	48686943	-
PRKDC	GRCh37/hg19	chr8	48689400	48689549	-
PRKDC	GRCh37/hg19	chr8	48690242	48690440	-
PRKDC	GRCh37/hg19	chr8	48691015	48691226	-
PRKDC	GRCh37/hg19	chr8	48691284	48691365	-
PRKDC	GRCh37/hg19	chr8	48691560	48691659	-
PRKDC	GRCh37/hg19	chr8	48694718	48694820	-
PRKDC	GRCh37/hg19	chr8	48694934	48695164	-
PRKDC	GRCh37/hg19	chr8	48696298	48696375	-
PRKDC	GRCh37/hg19	chr8	48697669	48697883	-
PRKDC	GRCh37/hg19	chr8	48701462	48701615	-
PRKDC	GRCh37/hg19	chr8	48701707	48701804	-
PRKDC	GRCh37/hg19	chr8	48706846	48707067	-
PRKDC	GRCh37/hg19	chr8	48710793	48710963	-
PRKDC	GRCh37/hg19	chr8	48711766	48711956	-
PRKDC	GRCh37/hg19	chr8	48713349	48713552	-
PRKDC	GRCh37/hg19	chr8	48715862	48716046	-
PRKDC	GRCh37/hg19	chr8	48719693	48719892	-
PRKDC	GRCh37/hg19	chr8	48730006	48730127	-
PRKDC	GRCh37/hg19	chr8	48731958	48732076	-
PRKDC	GRCh37/hg19	chr8	48733275	48733509	-
PRKDC	GRCh37/hg19	chr8	48734160	48734358	-
PRKDC	GRCh37/hg19	chr8	48736414	48736562	-
PRKDC	GRCh37/hg19	chr8	48739212	48739427	-
PRKDC	GRCh37/hg19	chr8	48740724	48740913	-
PRKDC	GRCh37/hg19	chr8	48743161	48743302	-
PRKDC	GRCh37/hg19	chr8	48744370	48744492	-
PRKDC	GRCh37/hg19	chr8	48746752	48746962	-
PRKDC	GRCh37/hg19	chr8	48748894	48749093	-
PRKDC	GRCh37/hg19	chr8	48749768	48749985	-
PRKDC	GRCh37/hg19	chr8	48751704	48751812	-
PRKDC	GRCh37/hg19	chr8	48752572	48752755	-
PRKDC	GRCh37/hg19	chr8	48761710	48761869	-
PRKDC	GRCh37/hg19	chr8	48761935	48762069	-
PRKDC	GRCh37/hg19	chr8	48765229	48765350	-
PRKDC	GRCh37/hg19	chr8	48766639	48766780	-
PRKDC	GRCh37/hg19	chr8	48767778	48767939	-
PRKDC	GRCh37/hg19	chr8	48769712	48769865	-
PRKDC	GRCh37/hg19	chr8	48771072	48771201	-
PRKDC	GRCh37/hg19	chr8	48771405	48771552	-
PRKDC	GRCh37/hg19	chr8	48772167	48772325	-
PRKDC	GRCh37/hg19	chr8	48773455	48773537	-
PRKDC	GRCh37/hg19	chr8	48774618	48774693	-

GENE-EXON	Reference	Chromosome	CHR_Start	CHR_End	STRAND
PRKDC	GRCh37/hg19	chr8	48774929	48775107	-
PRKDC	GRCh37/hg19	chr8	48775955	48776143	-
PRKDC	GRCh37/hg19	chr8	48777112	48777329	-
PRKDC	GRCh37/hg19	chr8	48790280	48790417	-
PRKDC	GRCh37/hg19	chr8	48792047	48792224	-
PRKDC	GRCh37/hg19	chr8	48793972	48794086	-
PRKDC	GRCh37/hg19	chr8	48794468	48794663	-
PRKDC	GRCh37/hg19	chr8	48798500	48798713	-
PRKDC	GRCh37/hg19	chr8	48800103	48800271	-
PRKDC	GRCh37/hg19	chr8	48801074	48801216	-
PRKDC	GRCh37/hg19	chr8	48801570	48801788	-
PRKDC	GRCh37/hg19	chr8	48802813	48803046	-
PRKDC	GRCh37/hg19	chr8	48805695	48805952	-
PRKDC	GRCh37/hg19	chr8	48809716	48809859	-
PRKDC	GRCh37/hg19	chr8	48811025	48811134	-
PRKDC	GRCh37/hg19	chr8	48812928	48813032	-
PRKDC	GRCh37/hg19	chr8	48815124	48815360	-
PRKDC	GRCh37/hg19	chr8	48817424	48817541	-
PRKDC	GRCh37/hg19	chr8	48824965	48825127	-
PRKDC	GRCh37/hg19	chr8	48826456	48826629	-
PRKDC	GRCh37/hg19	chr8	48827883	48827983	-
PRKDC	GRCh37/hg19	chr8	48830832	48830948	-
PRKDC	GRCh37/hg19	chr8	48839749	48839918	-
PRKDC	GRCh37/hg19	chr8	48840326	48840455	-
PRKDC	GRCh37/hg19	chr8	48841647	48841743	-
PRKDC	GRCh37/hg19	chr8	48842408	48842577	-
PRKDC	GRCh37/hg19	chr8	48843227	48843352	-
PRKDC	GRCh37/hg19	chr8	48845575	48845737	-
PRKDC	GRCh37/hg19	chr8	48846520	48846655	-
PRKDC	GRCh37/hg19	chr8	48847564	48847623	-
PRKDC	GRCh37/hg19	chr8	48848287	48848465	-
PRKDC	GRCh37/hg19	chr8	48848908	48849082	-
PRKDC	GRCh37/hg19	chr8	48852106	48852262	-
PRKDC	GRCh37/hg19	chr8	48855764	48855931	-
PRKDC	GRCh37/hg19	chr8	48856408	48856448	-
PRKDC	GRCh37/hg19	chr8	48856529	48856594	-
PRKDC	GRCh37/hg19	chr8	48866175	48866284	-
PRKDC	GRCh37/hg19	chr8	48866362	48866484	-
PRKDC	GRCh37/hg19	chr8	48866893	48867011	-
PRKDC	GRCh37/hg19	chr8	48868429	48868513	-
PRKDC	GRCh37/hg19	chr8	48869726	48869828	-
PRKDC	GRCh37/hg19	chr8	48869910	48869996	-
PRKDC	GRCh37/hg19	chr8	48872528	48872691	-
PTCH1	GRCh37/hg19	chr9	98209189	98209738	-
PTCH1	GRCh37/hg19	chr9	98211346	98211610	-
PTCH1	GRCh37/hg19	chr9	98212118	98212227	-
PTCH1	GRCh37/hg19	chr9	98215755	98215907	-
PTCH1	GRCh37/hg19	chr9	98218553	98218700	-
PTCH1	GRCh37/hg19	chr9	98220290	98220580	-
PTCH1	GRCh37/hg19	chr9	98221877	98222070	-
PTCH1	GRCh37/hg19	chr9	98224133	98224285	-
PTCH1	GRCh37/hg19	chr9	98229393	98229712	-
PTCH1	GRCh37/hg19	chr9	98231028	98231440	-
PTCH1	GRCh37/hg19	chr9	98232090	98232218	-
PTCH1	GRCh37/hg19	chr9	98238311	98238446	-
PTCH1	GRCh37/hg19	chr9	98239036	98239144	-

GENE-EXON	Reference	Chromosome	CHR_Start	CHR_End	STRAND
PTCH1	GRCh37/hg19	chr9	98239824	98239989	-
PTCH1	GRCh37/hg19	chr9	98240332	98240473	-
PTCH1	GRCh37/hg19	chr9	98241277	98241434	-
PTCH1	GRCh37/hg19	chr9	98242246	98242377	-
PTCH1	GRCh37/hg19	chr9	98242667	98242875	-
PTCH1	GRCh37/hg19	chr9	98244226	98244327	-
PTCH1	GRCh37/hg19	chr9	98244411	98244490	-
PTCH1	GRCh37/hg19	chr9	98247962	98248161	-
PTCH1	GRCh37/hg19	chr9	98268684	98268886	-
PTCH1	GRCh37/hg19	chr9	98270438	98270648	-
PTCH1	GRCh37/hg19	chr9	98278746	98278758	-
PTCH1	GRCh37/hg19	chr9	98278900	98279107	-
RAC1	GRCh37/hg19	chr7	6414362	6414406	+
RAC1	GRCh37/hg19	chr7	6426838	6426919	+
RAC1	GRCh37/hg19	chr7	6431550	6431677	+
RAC1	GRCh37/hg19	chr7	6438288	6438354	+
RAC1	GRCh37/hg19	chr7	6439752	6439824	+
RAC1	GRCh37/hg19	chr7	6441494	6441663	+
RAC1	GRCh37/hg19	chr7	6441942	6442082	+
RAD50	GRCh37/hg19	chr5	131893012	131893150	+
RAD50	GRCh37/hg19	chr5	131894971	131895064	+
RAD50	GRCh37/hg19	chr5	131911464	131911625	+
RAD50	GRCh37/hg19	chr5	131915004	131915199	+
RAD50	GRCh37/hg19	chr5	131915549	131915763	+
RAD50	GRCh37/hg19	chr5	131923249	131923387	+
RAD50	GRCh37/hg19	chr5	131923611	131923786	+
RAD50	GRCh37/hg19	chr5	131924374	131924577	+
RAD50	GRCh37/hg19	chr5	131925318	131925534	+
RAD50	GRCh37/hg19	chr5	131926911	131927103	+
RAD50	GRCh37/hg19	chr5	131927564	131927731	+
RAD50	GRCh37/hg19	chr5	131930556	131930741	+
RAD50	GRCh37/hg19	chr5	131931260	131931507	+
RAD50	GRCh37/hg19	chr5	131938987	131939186	+
RAD50	GRCh37/hg19	chr5	131939607	131939743	+
RAD50	GRCh37/hg19	chr5	131940493	131940696	+
RAD50	GRCh37/hg19	chr5	131944302	131944422	+
RAD50	GRCh37/hg19	chr5	131944804	131944906	+
RAD50	GRCh37/hg19	chr5	131944970	131945093	+
RAD50	GRCh37/hg19	chr5	131951690	131951827	+
RAD50	GRCh37/hg19	chr5	131953757	131953991	+
RAD50	GRCh37/hg19	chr5	131972802	131972897	+
RAD50	GRCh37/hg19	chr5	131973768	131973920	+
RAD50	GRCh37/hg19	chr5	131976359	131976502	+
RAD50	GRCh37/hg19	chr5	131977865	131978061	+
RIT1	GRCh37/hg19	chr1	155870174	155870414	-
RIT1	GRCh37/hg19	chr1	155874097	155874298	-
RIT1	GRCh37/hg19	chr1	155874517	155874600	-
RIT1	GRCh37/hg19	chr1	155880236	155880302	-
RIT1	GRCh37/hg19	chr1	155880442	155880600	-
RIT1	GRCh37/hg19	chr1	155880664	155880681	-
RUNX1	GRCh37/hg19	chr21	36164427	36164912	-
RUNX1	GRCh37/hg19	chr21	36171593	36171764	-
RUNX1	GRCh37/hg19	chr21	36193960	36193998	-
RUNX1	GRCh37/hg19	chr21	36206702	36206903	-
RUNX1	GRCh37/hg19	chr21	36231766	36231880	-
RUNX1	GRCh37/hg19	chr21	36252849	36253015	-

GENE-EXON	Reference	Chromosome	CHR_Start	CHR_End	STRAND
RUNX1	GRCh37/hg19	chr21	36259135	36259414	-
RUNX1	GRCh37/hg19	chr21	36265217	36265265	-
RUNX1	GRCh37/hg19	chr21	36421134	36421201	-
RUNX3	GRCh37/hg19	chr1	25228608	25229162	-
RUNX3	GRCh37/hg19	chr1	25233745	25233913	-
RUNX3	GRCh37/hg19	chr1	25245726	25245840	-
RUNX3	GRCh37/hg19	chr1	25254060	25254226	-
RUNX3	GRCh37/hg19	chr1	25256073	25256364	-
RUNX3	GRCh37/hg19	chr1	25291000	25291067	-
SDHA	GRCh37/hg19	chr5	218466	218538	+
SDHA	GRCh37/hg19	chr5	223592	223688	+
SDHA	GRCh37/hg19	chr5	224470	224641	+
SDHA	GRCh37/hg19	chr5	225529	225682	+
SDHA	GRCh37/hg19	chr5	225993	226167	+
SDHA	GRCh37/hg19	chr5	228295	228453	+
SDHA	GRCh37/hg19	chr5	230986	231120	+
SDHA	GRCh37/hg19	chr5	233587	233765	+
SDHA	GRCh37/hg19	chr5	235254	235459	+
SDHA	GRCh37/hg19	chr5	236538	236719	+
SDHA	GRCh37/hg19	chr5	240468	240596	+
SDHA	GRCh37/hg19	chr5	251102	251223	+
SDHA	GRCh37/hg19	chr5	251448	251588	+
SDHA	GRCh37/hg19	chr5	254503	254626	+
SDHA	GRCh37/hg19	chr5	256444	256540	+
SDHB	GRCh37/hg19	chr1	17345371	17345458	-
SDHB	GRCh37/hg19	chr1	17349098	17349230	-
SDHB	GRCh37/hg19	chr1	17350463	17350574	-
SDHB	GRCh37/hg19	chr1	17354239	17354365	-
SDHB	GRCh37/hg19	chr1	17355090	17355236	-
SDHB	GRCh37/hg19	chr1	17359550	17359645	-
SDHB	GRCh37/hg19	chr1	17371251	17371388	-
SDHB	GRCh37/hg19	chr1	17380438	17380519	-
SDHC	GRCh37/hg19	chr1	161284191	161284220	+
SDHC	GRCh37/hg19	chr1	161293399	161293465	+
SDHC	GRCh37/hg19	chr1	161298181	161298292	+
SDHC	GRCh37/hg19	chr1	161310379	161310450	+
SDHC	GRCh37/hg19	chr1	161326462	161326635	+
SDHC	GRCh37/hg19	chr1	161332114	161332335	+
SDHD	GRCh37/hg19	chr11	111957627	111957688	+
SDHD	GRCh37/hg19	chr11	111958576	111958702	+
SDHD	GRCh37/hg19	chr11	111959586	111959740	+
SDHD	GRCh37/hg19	chr11	111963799	111963926	+
SDHD	GRCh37/hg19	chr11	111965524	111965699	+
SETD2	GRCh37/hg19	chr3	47058578	47058749	-
SETD2	GRCh37/hg19	chr3	47059123	47059234	-
SETD2	GRCh37/hg19	chr3	47061245	47061335	-
SETD2	GRCh37/hg19	chr3	47079151	47079272	-
SETD2	GRCh37/hg19	chr3	47084046	47084195	-
SETD2	GRCh37/hg19	chr3	47087972	47088116	-
SETD2	GRCh37/hg19	chr3	47098306	47098985	-
SETD2	GRCh37/hg19	chr3	47103648	47103841	-
SETD2	GRCh37/hg19	chr3	47108555	47108613	-
SETD2	GRCh37/hg19	chr3	47125205	47125877	-
SETD2	GRCh37/hg19	chr3	47127680	47127809	-
SETD2	GRCh37/hg19	chr3	47129598	47129742	-
SETD2	GRCh37/hg19	chr3	47139440	47139576	-

GENE-EXON	Reference	Chromosome	CHR_Start	CHR_End	STRAND
SETD2	GRCh37/hg19	chr3	47142943	47143050	-
SETD2	GRCh37/hg19	chr3	47144831	47144918	-
SETD2	GRCh37/hg19	chr3	47147482	47147615	-
SETD2	GRCh37/hg19	chr3	47155361	47155499	-
SETD2	GRCh37/hg19	chr3	47158108	47158249	-
SETD2	GRCh37/hg19	chr3	47161667	47166043	-
SETD2	GRCh37/hg19	chr3	47168133	47168158	-
SETD2	GRCh37/hg19	chr3	47205339	47205419	-
SMAD2	GRCh37/hg19	chr18	45368193	45368326	-
SMAD2	GRCh37/hg19	chr18	45371706	45371860	-
SMAD2	GRCh37/hg19	chr18	45372029	45372176	-
SMAD2	GRCh37/hg19	chr18	45374841	45375063	-
SMAD2	GRCh37/hg19	chr18	45377640	45377703	-
SMAD2	GRCh37/hg19	chr18	45391425	45391509	-
SMAD2	GRCh37/hg19	chr18	45394689	45394833	-
SMAD2	GRCh37/hg19	chr18	45395609	45395812	-
SMAD2	GRCh37/hg19	chr18	45396841	45396940	-
SMAD2	GRCh37/hg19	chr18	45422887	45423132	-
SMAD3	GRCh37/hg19	chr15	67358488	67358703	+
SMAD3	GRCh37/hg19	chr15	67430360	67430443	+
SMAD3	GRCh37/hg19	chr15	67457228	67457431	+
SMAD3	GRCh37/hg19	chr15	67457586	67457727	+
SMAD3	GRCh37/hg19	chr15	67459112	67459196	+
SMAD3	GRCh37/hg19	chr15	67462887	67462947	+
SMAD3	GRCh37/hg19	chr15	67473574	67473796	+
SMAD3	GRCh37/hg19	chr15	67477060	67477207	+
SMAD3	GRCh37/hg19	chr15	67479698	67479852	+
SMAD3	GRCh37/hg19	chr15	67482746	67482879	+
SMAD4	GRCh37/hg19	chr18	48573412	48573670	+
SMAD4	GRCh37/hg19	chr18	48575051	48575235	+
SMAD4	GRCh37/hg19	chr18	48575660	48575699	+
SMAD4	GRCh37/hg19	chr18	48581146	48581368	+
SMAD4	GRCh37/hg19	chr18	48584490	48584619	+
SMAD4	GRCh37/hg19	chr18	48584705	48584831	+
SMAD4	GRCh37/hg19	chr18	48586231	48586291	+
SMAD4	GRCh37/hg19	chr18	48591788	48591981	+
SMAD4	GRCh37/hg19	chr18	48593384	48593562	+
SMAD4	GRCh37/hg19	chr18	48603003	48603151	+
SMAD4	GRCh37/hg19	chr18	48604621	48604842	+
SNX31	GRCh37/hg19	chr8	101586088	101586193	-
SNX31	GRCh37/hg19	chr8	101589242	101589308	-
SNX31	GRCh37/hg19	chr8	101596334	101596421	-
SNX31	GRCh37/hg19	chr8	101601089	101601212	-
SNX31	GRCh37/hg19	chr8	101608862	101609075	-
SNX31	GRCh37/hg19	chr8	101612572	101612674	-
SNX31	GRCh37/hg19	chr8	101620717	101620796	-
SNX31	GRCh37/hg19	chr8	101624223	101624320	-
SNX31	GRCh37/hg19	chr8	101625218	101625318	-
SNX31	GRCh37/hg19	chr8	101629843	101629963	-
SNX31	GRCh37/hg19	chr8	101642550	101642624	-
SNX31	GRCh37/hg19	chr8	101648120	101648244	-
SNX31	GRCh37/hg19	chr8	101661497	101661581	-
SNX31	GRCh37/hg19	chr8	101661672	101661747	-
SPOP	GRCh37/hg19	chr17	47677735	47677889	-
SPOP	GRCh37/hg19	chr17	47679222	47679374	-
SPOP	GRCh37/hg19	chr17	47684607	47684739	-

GENE-EXON	Reference	Chromosome	CHR_Start	CHR_End	STRAND
SPOP	GRCh37/hg19	chr17	47685231	47685296	-
SPOP	GRCh37/hg19	chr17	47688637	47688824	-
SPOP	GRCh37/hg19	chr17	47696338	47696475	-
SPOP	GRCh37/hg19	chr17	47696591	47696752	-
SPOP	GRCh37/hg19	chr17	47699303	47699434	-
SPOP	GRCh37/hg19	chr17	47700090	47700177	-
T	GRCh37/hg19	chr6	166571798	166572081	-
T	GRCh37/hg19	chr6	166574320	166574459	-
T	GRCh37/hg19	chr6	166575930	166576113	-
T	GRCh37/hg19	chr6	166578088	166578159	-
T	GRCh37/hg19	chr6	166578283	166578354	-
T	GRCh37/hg19	chr6	166579189	166579333	-
T	GRCh37/hg19	chr6	166580075	166580349	-
T	GRCh37/hg19	chr6	166580869	166581084	-
TBX3	GRCh37/hg19	chr12	115109641	115110112	-
TBX3	GRCh37/hg19	chr12	115111965	115112645	-
TBX3	GRCh37/hg19	chr12	115114113	115114280	-
TBX3	GRCh37/hg19	chr12	115115380	115115466	-
TBX3	GRCh37/hg19	chr12	115117305	115117461	-
TBX3	GRCh37/hg19	chr12	115117713	115117782	-
TBX3	GRCh37/hg19	chr12	115118679	115118956	-
TBX3	GRCh37/hg19	chr12	115120612	115121010	-
TERT	GRCh37/hg19	chr5	1253838	1253951	-
TERT	GRCh37/hg19	chr5	1254478	1254625	-
TERT	GRCh37/hg19	chr5	1255397	1255531	-
TERT	GRCh37/hg19	chr5	1258708	1258779	-
TERT	GRCh37/hg19	chr5	1260584	1260720	-
TERT	GRCh37/hg19	chr5	1264514	1264712	-
TERT	GRCh37/hg19	chr5	1266574	1266655	-
TERT	GRCh37/hg19	chr5	1268630	1268753	-
TERT	GRCh37/hg19	chr5	1271229	1271324	-
TERT	GRCh37/hg19	chr5	1272295	1272400	-
TERT	GRCh37/hg19	chr5	1278751	1278916	-
TERT	GRCh37/hg19	chr5	1279401	1279590	-
TERT	GRCh37/hg19	chr5	1280268	1280458	-
TERT	GRCh37/hg19	chr5	1282539	1282744	-
TERT	GRCh37/hg19	chr5	1293423	1294786	-
TERT	GRCh37/hg19	chr5	1294881	1295109	-
TGFBR2	GRCh37/hg19	chr3	30648371	30648474	+
TGFBR2	GRCh37/hg19	chr3	30664686	30664770	+
TGFBR2	GRCh37/hg19	chr3	30686234	30686412	+
TGFBR2	GRCh37/hg19	chr3	30691757	30691957	+
TGFBR2	GRCh37/hg19	chr3	30713125	30713934	+
TGFBR2	GRCh37/hg19	chr3	30715592	30715743	+
TGFBR2	GRCh37/hg19	chr3	30729871	30730008	+
TGFBR2	GRCh37/hg19	chr3	30732907	30733096	+
TNF	GRCh37/hg19	chr6	31543514	31543709	+
TNF	GRCh37/hg19	chr6	31544306	31544361	+
TNF	GRCh37/hg19	chr6	31544539	31544596	+
TNF	GRCh37/hg19	chr6	31544888	31545319	+
TSC1	GRCh37/hg19	chr9	135771617	135772146	-
TSC1	GRCh37/hg19	chr9	135772566	135772737	-
TSC1	GRCh37/hg19	chr9	135772805	135773002	-
TSC1	GRCh37/hg19	chr9	135776097	135776229	-
TSC1	GRCh37/hg19	chr9	135776971	135777091	-
TSC1	GRCh37/hg19	chr9	135777987	135778179	-

GENE-EXON	Reference	Chromosome	CHR_Start	CHR_End	STRAND
TSC1	GRCh37/hg19	chr9	135779033	135779209	-
TSC1	GRCh37/hg19	chr9	135779793	135779846	-
TSC1	GRCh37/hg19	chr9	135780963	135781531	-
TSC1	GRCh37/hg19	chr9	135782113	135782227	-
TSC1	GRCh37/hg19	chr9	135782683	135782762	-
TSC1	GRCh37/hg19	chr9	135785953	135786084	-
TSC1	GRCh37/hg19	chr9	135786384	135786505	-
TSC1	GRCh37/hg19	chr9	135786835	135786960	-
TSC1	GRCh37/hg19	chr9	135787664	135787849	-
TSC1	GRCh37/hg19	chr9	135796745	135796828	-
TSC1	GRCh37/hg19	chr9	135797201	135797365	-
TSC1	GRCh37/hg19	chr9	135798730	135798884	-
TSC1	GRCh37/hg19	chr9	135800969	135801131	-
TSC1	GRCh37/hg19	chr9	135802583	135802696	-
TSC1	GRCh37/hg19	chr9	135804149	135804264	-
TSC2	GRCh37/hg19	chr16	2098612	2098759	+
TSC2	GRCh37/hg19	chr16	2100396	2100492	+
TSC2	GRCh37/hg19	chr16	2103338	2103458	+
TSC2	GRCh37/hg19	chr16	2104292	2104446	+
TSC2	GRCh37/hg19	chr16	2105398	2105525	+
TSC2	GRCh37/hg19	chr16	2106192	2106250	+
TSC2	GRCh37/hg19	chr16	2106640	2106775	+
TSC2	GRCh37/hg19	chr16	2107101	2107184	+
TSC2	GRCh37/hg19	chr16	2108743	2108879	+
TSC2	GRCh37/hg19	chr16	2110666	2110819	+
TSC2	GRCh37/hg19	chr16	2111867	2112014	+
TSC2	GRCh37/hg19	chr16	2112493	2112606	+
TSC2	GRCh37/hg19	chr16	2112968	2113059	+
TSC2	GRCh37/hg19	chr16	2114268	2114433	+
TSC2	GRCh37/hg19	chr16	2115515	2115641	+
TSC2	GRCh37/hg19	chr16	2120452	2120584	+
TSC2	GRCh37/hg19	chr16	2121506	2121622	+
TSC2	GRCh37/hg19	chr16	2121780	2121940	+
TSC2	GRCh37/hg19	chr16	2122237	2122369	+
TSC2	GRCh37/hg19	chr16	2122845	2122989	+
TSC2	GRCh37/hg19	chr16	2124196	2124395	+
TSC2	GRCh37/hg19	chr16	2125795	2125898	+
TSC2	GRCh37/hg19	chr16	2126064	2126176	+
TSC2	GRCh37/hg19	chr16	2126487	2126591	+
TSC2	GRCh37/hg19	chr16	2127594	2127732	+
TSC2	GRCh37/hg19	chr16	2129028	2129202	+
TSC2	GRCh37/hg19	chr16	2129272	2129434	+
TSC2	GRCh37/hg19	chr16	2129553	2129675	+
TSC2	GRCh37/hg19	chr16	2130161	2130383	+
TSC2	GRCh37/hg19	chr16	2131591	2131804	+
TSC2	GRCh37/hg19	chr16	2132432	2132510	+
TSC2	GRCh37/hg19	chr16	2133691	2133822	+
TSC2	GRCh37/hg19	chr16	2134224	2134721	+
TSC2	GRCh37/hg19	chr16	2134947	2135032	+
TSC2	GRCh37/hg19	chr16	2135226	2135328	+
TSC2	GRCh37/hg19	chr16	2136189	2136385	+
TSC2	GRCh37/hg19	chr16	2136728	2136877	+
TSC2	GRCh37/hg19	chr16	2137859	2137947	+
TSC2	GRCh37/hg19	chr16	2138044	2138145	+
TSC2	GRCh37/hg19	chr16	2138223	2138331	+
TSC2	GRCh37/hg19	chr16	2138442	2138616	+

GENE-EXON	Reference	Chromosome	CHR_Start	CHR_End	STRAND
TXNRD3	GRCh37/hg19	chr3	126326743	126326821	-
TXNRD3	GRCh37/hg19	chr3	126327337	126327481	-
TXNRD3	GRCh37/hg19	chr3	126329875	126329980	-
TXNRD3	GRCh37/hg19	chr3	126334193	126334310	-
TXNRD3	GRCh37/hg19	chr3	126340580	126340746	-
TXNRD3	GRCh37/hg19	chr3	126341302	126341388	-
TXNRD3	GRCh37/hg19	chr3	126348217	126348319	-
TXNRD3	GRCh37/hg19	chr3	126349550	126349785	-
TXNRD3	GRCh37/hg19	chr3	126350602	126350727	-
TXNRD3	GRCh37/hg19	chr3	126352747	126352899	-
TXNRD3	GRCh37/hg19	chr3	126360870	126360999	-
TXNRD3	GRCh37/hg19	chr3	126362819	126362901	-
TXNRD3	GRCh37/hg19	chr3	126363135	126363249	-
TXNRD3	GRCh37/hg19	chr3	126364949	126365068	-
TXNRD3	GRCh37/hg19	chr3	126366074	126366144	-
TXNRD3	GRCh37/hg19	chr3	126373586	126373838	-
VHL	GRCh37/hg19	chr3	10183527	10183876	+
VHL	GRCh37/hg19	chr3	10188193	10188325	+
VHL	GRCh37/hg19	chr3	10191466	10191654	+
WT1	GRCh37/hg19	chr11	32410599	32410730	+
WT1	GRCh37/hg19	chr11	32413513	32413615	+
WT1	GRCh37/hg19	chr11	32414207	32414306	+
WT1	GRCh37/hg19	chr11	32417798	32417958	+
WT1	GRCh37/hg19	chr11	32421489	32421595	+
WT1	GRCh37/hg19	chr11	32438031	32438091	+
WT1	GRCh37/hg19	chr11	32439118	32439205	+
WT1	GRCh37/hg19	chr11	32449497	32449609	+
WT1	GRCh37/hg19	chr11	32450038	32450170	+
WT1	GRCh37/hg19	chr11	32452071	32452090	+
WT1	GRCh37/hg19	chr11	32456241	32456896	+
MPL_10	GRCh37/hg19	chr1	43814934	43815030	+
NRAS_4	GRCh37/hg19	chr1	115252190	115252349	-
NRAS_3	GRCh37/hg19	chr1	115256421	115256599	-
NRAS_2	GRCh37/hg19	chr1	115258671	115258798	-
DDR2_10	GRCh37/hg19	chr1	162740092	162740302	+
DDR2_11	GRCh37/hg19	chr1	162741814	162742037	+
DDR2_12	GRCh37/hg19	chr1	162743259	162743386	+
DDR2_13	GRCh37/hg19	chr1	162745442	162745633	+
DDR2_14	GRCh37/hg19	chr1	162745926	162746160	+
DDR2_15	GRCh37/hg19	chr1	162748370	162748519	+
DDR2_16	GRCh37/hg19	chr1	162749902	162750022	+
RET_10	GRCh37/hg19	chr10	43609004	43609123	+
RET_11	GRCh37/hg19	chr10	43609928	43610184	+
RET_13	GRCh37/hg19	chr10	43613821	43613928	+
RET_15	GRCh37/hg19	chr10	43615529	43615651	+
RET_16	GRCh37/hg19	chr10	43617394	43617464	+
PTEN_1	GRCh37/hg19	chr10	89624208	89624305	+
PTEN_3	GRCh37/hg19	chr10	89685270	89685314	+
PTEN_5	GRCh37/hg19	chr10	89692770	89693008	+
PTEN_6	GRCh37/hg19	chr10	89711875	89712016	+
PTEN_7	GRCh37/hg19	chr10	89717610	89717776	+
PTEN_8	GRCh37/hg19	chr10	89720651	89720875	+
PTEN_9	GRCh37/hg19	chr10	89725044	89725224	+
FGFR2_15	GRCh37/hg19	chr10	123246868	123246938	-
FGFR2_14	GRCh37/hg19	chr10	123247505	123247627	-
FGFR2_13	GRCh37/hg19	chr10	123256046	123256236	-

GENE-EXON	Reference	Chromosome	CHR_Start	CHR_End	STRAND
FGFR2_12	GRCh37/hg19	chr10	123258009	123258119	-
FGFR2_11	GRCh37/hg19	chr10	123260340	123260461	-
FGFR2_10	GRCh37/hg19	chr10	123263304	123263455	-
FGFR2_9	GRCh37/hg19	chr10	123274631	123274833	-
FGFR2_8	GRCh37/hg19	chr10	123276833	123276977	-
FGFR2_7	GRCh37/hg19	chr10	123279493	123279683	-
HRAS_4	GRCh37/hg19	chr11	533453	533612	-
HRAS_3	GRCh37/hg19	chr11	533766	533944	-
HRAS_2	GRCh37/hg19	chr11	534212	534375	-
ATM_8	GRCh37/hg19	chr11	108117691	108117854	+
ATM_9	GRCh37/hg19	chr11	108119660	108119829	+
ATM_12	GRCh37/hg19	chr11	108123544	108123639	+
ATM_17	GRCh37/hg19	chr11	108137898	108138069	+
ATM_26	GRCh37/hg19	chr11	108154954	108155200	+
ATM_34	GRCh37/hg19	chr11	108170441	108170612	+
ATM_35	GRCh37/hg19	chr11	108172375	108172516	+
ATM_36	GRCh37/hg19	chr11	108173580	108173756	+
ATM_39	GRCh37/hg19	chr11	108180887	108181042	+
ATM_50	GRCh37/hg19	chr11	108200941	108201148	+
ATM_54	GRCh37/hg19	chr11	108204613	108204695	+
ATM_55	GRCh37/hg19	chr11	108205696	108205836	+
ATM_56	GRCh37/hg19	chr11	108206572	108206688	+
ATM_59	GRCh37/hg19	chr11	108218006	108218092	+
ATM_61	GRCh37/hg19	chr11	108225538	108225601	+
ATM_63	GRCh37/hg19	chr11	108236052	108236232	+
KRAS_4	GRCh37/hg19	chr12	25378548	25378707	-
KRAS_3	GRCh37/hg19	chr12	25380168	25380346	-
KRAS_2	GRCh37/hg19	chr12	25398208	25398329	-
ARID2_15	GRCh37/hg19	chr12	46243819	46246679	+
PTPN11_3	GRCh37/hg19	chr12	112888122	112888316	+
PTPN11_13	GRCh37/hg19	chr12	112926828	112926979	+
HNF1A_3	GRCh37/hg19	chr12	121431323	121431509	+
HNF1A_4	GRCh37/hg19	chr12	121431967	121432208	+
FLT3_20	GRCh37/hg19	chr13	28592604	28592726	-
FLT3_16	GRCh37/hg19	chr13	28602315	28602425	-
FLT3_14	GRCh37/hg19	chr13	28608219	28608351	-
FLT3_11	GRCh37/hg19	chr13	28610072	28610180	-
RB1_4	GRCh37/hg19	chr13	48919216	48919335	+
RB1_6	GRCh37/hg19	chr13	48923092	48923159	+
RB1_10	GRCh37/hg19	chr13	48941630	48941739	+
RB1_11	GRCh37/hg19	chr13	48942663	48942740	+
RB1_14	GRCh37/hg19	chr13	48953730	48953786	+
RB1_17	GRCh37/hg19	chr13	48955383	48955579	+
RB1_18	GRCh37/hg19	chr13	49027129	49027247	+
RB1_20	GRCh37/hg19	chr13	49033824	49033969	+
RB1_21	GRCh37/hg19	chr13	49037867	49037971	+
RB1_22	GRCh37/hg19	chr13	49039134	49039247	+
AKT_5	GRCh37/hg19	chr14	105241413	105241544	-
AKT_2	GRCh37/hg19	chr14	105246425	105246553	-
MEK1_2	GRCh37/hg19	chr15	66727365	66727575	+
MEK1_3	GRCh37/hg19	chr15	66729084	66729230	+
MEK1_4	GRCh37/hg19	chr15	66735618	66735695	+
MEK1_5	GRCh37/hg19	chr15	66736994	66737045	+
MEK1_6	GRCh37/hg19	chr15	66774093	66774217	+
MEK1_7	GRCh37/hg19	chr15	66777328	66777529	+
MEK1_8	GRCh37/hg19	chr15	66779566	66779630	+

GENE-EXON	Reference	Chromosome	CHR_Start	CHR_End	STRAND
MEK1_9	GRCh37/hg19	chr15	66781553	66781614	+
MEK1_10	GRCh37/hg19	chr15	66782056	66782101	+
MEK1_11	GRCh37/hg19	chr15	66782840	66782959	+
IDH2_4	GRCh37/hg19	chr15	90631819	90631979	-
CDH1_3	GRCh37/hg19	chr16	68835573	68835796	+
CDH1_8	GRCh37/hg19	chr16	68846038	68846166	+
CDH1_9	GRCh37/hg19	chr16	68847216	68847398	+
TP53_10	GRCh37/hg19	chr17	7573927	7574033	-
TP53_9	GRCh37/hg19	chr17	7576853	7576926	-
TP53_8	GRCh37/hg19	chr17	7577019	7577155	-
TP53_7	GRCh37/hg19	chr17	7577499	7577608	-
TP53_6	GRCh37/hg19	chr17	7578177	7578289	-
TP53_5	GRCh37/hg19	chr17	7578371	7578554	-
TP53_4	GRCh37/hg19	chr17	7579312	7579590	-
TP53_2	GRCh37/hg19	chr17	7579839	7579940	-
MEK4_3	GRCh37/hg19	chr17	11958206	11958308	+
MEK4_4	GRCh37/hg19	chr17	11984673	11984847	+
MEK4_5	GRCh37/hg19	chr17	11998892	11999011	+
MEK4_6	GRCh37/hg19	chr17	12011107	12011226	+
MEK4_7	GRCh37/hg19	chr17	12013692	12013743	+
MEK4_8	GRCh37/hg19	chr17	12016550	12016677	+
MEK4_9	GRCh37/hg19	chr17	12028611	12028688	+
MEK4_10	GRCh37/hg19	chr17	12032456	12032604	+
HER2_17	GRCh37/hg19	chr17	37879572	37879710	+
HER2_18	GRCh37/hg19	chr17	37879791	37879913	+
HER2_19	GRCh37/hg19	chr17	37880165	37880263	+
HER2_20	GRCh37/hg19	chr17	37880979	37881164	+
HER2_21	GRCh37/hg19	chr17	37881302	37881457	+
HER2_22	GRCh37/hg19	chr17	37881580	37881655	+
HER2_23	GRCh37/hg19	chr17	37881960	37882106	+
LKB1_1	GRCh37/hg19	chr19	1206880	1207202	+
LKB1_4	GRCh37/hg19	chr19	1220372	1220504	+
LKB1_5	GRCh37/hg19	chr19	1220580	1220716	+
LKB1_6	GRCh37/hg19	chr19	1221212	1221339	+
LKB1_8	GRCh37/hg19	chr19	1222984	1223171	+
GNA11_4	GRCh37/hg19	chr19	3114942	3115070	+
GNA11_5	GRCh37/hg19	chr19	3118922	3119051	+
JAK3_15	GRCh37/hg19	chr19	17945661	17945812	-
JAK3_12	GRCh37/hg19	chr19	17947938	17948022	-
JAK3_3	GRCh37/hg19	chr19	17954189	17954300	-
ALK_25	GRCh37/hg19	chr2	29432652	29432744	-
ALK_24	GRCh37/hg19	chr2	29436850	29436947	-
ALK_23	GRCh37/hg19	chr2	29443572	29443701	-
ALK_22	GRCh37/hg19	chr2	29445210	29445274	-
ALK_21	GRCh37/hg19	chr2	29445383	29445473	-
IDH1_4	GRCh37/hg19	chr2	209113093	209113384	-
HER4_23	GRCh37/hg19	chr2	212288880	212289026	-
HER4_15	GRCh37/hg19	chr2	212530048	212530202	-
HER4_9	GRCh37/hg19	chr2	212576775	212576901	-
HER4_8	GRCh37/hg19	chr2	212578260	212578373	-
HER4_7	GRCh37/hg19	chr2	212587118	212587259	-
HER4_6	GRCh37/hg19	chr2	212589801	212589919	-
HER4_4	GRCh37/hg19	chr2	212652750	212652884	-
HER4_3	GRCh37/hg19	chr2	212812155	212812341	-
SRC_14	GRCh37/hg19	chr20	36031574	36031813	+
GNAS_8	GRCh37/hg19	chr20	57484405	57484478	+

GENE-EXON	Reference	Chromosome	CHR_Start	CHR_End	STRAND
GNAS_9	GRCh37/hg19	chr20	57484576	57484634	+
SMARCB1_2	GRCh37/hg19	chr22	24133943	24134081	+
SMARCB1_4	GRCh37/hg19	chr22	24143131	24143268	+
SMARCB1_5	GRCh37/hg19	chr22	24145482	24145609	+
SMARCB1_9	GRCh37/hg19	chr22	24176328	24176387	+
MLH1_12	GRCh37/hg19	chr3	37067128	37067498	+
CTNNB1_3	GRCh37/hg19	chr3	41266017	41266244	+
PIK3CA_1	GRCh37/hg19	chr3	178916612	178916965	+
PIK3CA_2	GRCh37/hg19	chr3	178917478	178917687	+
PIK3CA_4	GRCh37/hg19	chr3	178921332	178921577	+
PIK3CA_6	GRCh37/hg19	chr3	178927383	178927488	+
PIK3CA_7	GRCh37/hg19	chr3	178927974	178928126	+
PIK3CA_9	GRCh37/hg19	chr3	178935998	178936122	+
PIK3CA_13	GRCh37/hg19	chr3	178938774	178938945	+
PIK3CA_18	GRCh37/hg19	chr3	178947792	178947909	+
PIK3CA_20	GRCh37/hg19	chr3	178951882	178952161	+
FGFR3_7	GRCh37/hg19	chr4	1803562	1803752	+
FGFR3_9	GRCh37/hg19	chr4	1806057	1806247	+
FGFR3_14	GRCh37/hg19	chr4	1807778	1807900	+
FGFR3_16	GRCh37/hg19	chr4	1808273	1808410	+
FGFR3_18	GRCh37/hg19	chr4	1808843	1809022	+
PDGFRA_10	GRCh37/hg19	chr4	55139704	55139897	+
PDGFRA_12	GRCh37/hg19	chr4	55141008	55141140	+
PDGFRA_13	GRCh37/hg19	chr4	55143555	55143659	+
PDGFRA_14	GRCh37/hg19	chr4	55144063	55144173	+
PDGFRA_15	GRCh37/hg19	chr4	55144529	55144682	+
PDGFRA_18	GRCh37/hg19	chr4	55152038	55152100	+
KIT_2	GRCh37/hg19	chr4	55561678	55561947	+
KIT_9	GRCh37/hg19	chr4	55592023	55592216	+
KIT_10	GRCh37/hg19	chr4	55593384	55593490	+
KIT_11	GRCh37/hg19	chr4	55593585	55593710	+
KIT_13	GRCh37/hg19	chr4	55594177	55594287	+
KIT_14	GRCh37/hg19	chr4	55595501	55595651	+
KIT_15	GRCh37/hg19	chr4	55597494	55597585	+
KIT_17	GRCh37/hg19	chr4	55599236	55599358	+
KIT_18	GRCh37/hg19	chr4	55602664	55602775	+
KDR_30	GRCh37/hg19	chr4	55946091	55946330	-
KDR_27	GRCh37/hg19	chr4	55953774	55953925	-
KDR_26	GRCh37/hg19	chr4	55955035	55955140	-
KDR_21	GRCh37/hg19	chr4	55960969	55961122	-
KDR_19	GRCh37/hg19	chr4	55962396	55962509	-
KDR_11	GRCh37/hg19	chr4	55972854	55972977	-
KDR_7	GRCh37/hg19	chr4	55979471	55979648	-
KDR_6	GRCh37/hg19	chr4	55980293	55980432	-
FBXW7_11	GRCh37/hg19	chr4	153245336	153245546	-
FBXW7_10	GRCh37/hg19	chr4	153247158	153247383	-
FBXW7_9	GRCh37/hg19	chr4	153249360	153249541	-
FBXW7_8	GRCh37/hg19	chr4	153250824	153250937	-
FBXW7_5	GRCh37/hg19	chr4	153258954	153259088	-
APC_15_HSPT	GRCh37/hg19	chr5	112173872	112176035	+
CSF1R_22	GRCh37/hg19	chr5	149433608	149433787	-
CSF1R_7	GRCh37/hg19	chr5	149452864	149453056	-
NPM1_11	GRCh37/hg19	chr5	170837531	170837590	+
EGFR_3	GRCh37/hg19	chr7	55210998	55211181	+
EGFR_7	GRCh37/hg19	chr7	55221704	55221845	+
EGFR_15	GRCh37/hg19	chr7	55232973	55233130	+

GENE-EXON	Reference	Chromosome	CHR_Start	CHR_End	STRAND
EGFR_17	GRCh37/hg19	chr7	55240676	55240817	+
EGFR_18	GRCh37/hg19	chr7	55241614	55241736	+
EGFR_19	GRCh37/hg19	chr7	55242436	55242485	+
EGFR_20	GRCh37/hg19	chr7	55248986	55249171	+
EGFR_21	GRCh37/hg19	chr7	55259412	55259567	+
EGFR_22	GRCh37/hg19	chr7	55260459	55260534	+
MET_2	GRCh37/hg19	chr7	116339125	116340338	+
MET_11	GRCh37/hg19	chr7	116403104	116403322	+
MET_14	GRCh37/hg19	chr7	116411903	116412043	+
MET_15	GRCh37/hg19	chr7	116414935	116415165	+
MET_16	GRCh37/hg19	chr7	116417443	116417523	+
MET_17	GRCh37/hg19	chr7	116418830	116419011	+
MET_18	GRCh37/hg19	chr7	116422042	116422151	+
MET_19	GRCh37/hg19	chr7	116423358	116423523	+
SMO_3	GRCh37/hg19	chr7	128845044	128845253	+
SMO_5	GRCh37/hg19	chr7	128845991	128846210	+
SMO_6	GRCh37/hg19	chr7	128846305	128846428	+
SMO_9	GRCh37/hg19	chr7	128850204	128850389	+
SMO_11	GRCh37/hg19	chr7	128851477	128851611	+
BRAF_15	GRCh37/hg19	chr7	140453075	140453193	-
BRAF_11	GRCh37/hg19	chr7	140481376	140481493	-
EZH2_15	GRCh37/hg19	chr7	148508717	148508812	-
FGFR1_16	GRCh37/hg19	chr8	38271670	38271807	-
FGFR1_15	GRCh37/hg19	chr8	38272077	38272147	-
FGFR1_14	GRCh37/hg19	chr8	38272297	38272419	-
FGFR1_13	GRCh37/hg19	chr8	38273388	38273578	-
FGFR1_12	GRCh37/hg19	chr8	38274824	38274934	-
FGFR1_11	GRCh37/hg19	chr8	38275388	38275509	-
FGFR1_10	GRCh37/hg19	chr8	38275746	38275891	-
FGFR1_9	GRCh37/hg19	chr8	38277051	38277253	-
FGFR1_7	GRCh37/hg19	chr8	38282027	38282217	-
FGFR1_4	GRCh37/hg19	chr8	38285864	38285953	-
TACC1_5	GRCh37/hg19	chr8	38684686	38684893	+
TACC1_10	GRCh37/hg19	chr8	38699805	38699965	+
TACC1_11	GRCh37/hg19	chr8	38700807	38700913	+
JAK2_14	GRCh37/hg19	chr9	5073698	5073785	+
CDKN2A_2	GRCh37/hg19	chr9	21970901	21971207	-
GNAQ_5	GRCh37/hg19	chr9	80409379	80409508	-
GNAQ_4	GRCh37/hg19	chr9	80412436	80412564	-
PPP6C_8	GRCh37/hg19	chr9	127911960	127912200	-
PPP6C_7	GRCh37/hg19	chr9	127915812	127916021	-
PPP6C_6	GRCh37/hg19	chr9	127916185	127916264	-
PPP6C_5	GRCh37/hg19	chr9	127920520	127920661	-
PPP6C_4	GRCh37/hg19	chr9	127923120	127923185	-
ABL1_4	GRCh37/hg19	chr9	133738150	133738422	+
ABL1_5	GRCh37/hg19	chr9	133747516	133747600	+
ABL1_6	GRCh37/hg19	chr9	133748247	133748424	+
ABL1_7	GRCh37/hg19	chr9	133750255	133750439	+
NOTCH1_34	GRCh37/hg19	chr9	139390570	139392010	-
NOTCH1_27	GRCh37/hg19	chr9	139397634	139397782	-
NOTCH1_26	GRCh37/hg19	chr9	139399125	139399556	-
EGFR_1	GRCh37/hg19	chr7	55086948	55087058	+
EGFR_2	GRCh37/hg19	chr7	55209979	55210130	+
EGFR_3	GRCh37/hg19	chr7	55210998	55211181	+
EGFR_4	GRCh37/hg19	chr7	55214299	55214433	+
EGFR_5	GRCh37/hg19	chr7	55218987	55219055	+

GENE-EXON	Reference	Chromosome	CHR_Start	CHR_End	STRAND
EGFR_6	GRCh37/hg19	chr7	55220239	55220357	+
EGFR_7	GRCh37/hg19	chr7	55221704	55221845	+
EGFR_8	GRCh37/hg19	chr7	55223523	55223639	+
EGFR_9	GRCh37/hg19	chr7	55224226	55224352	+
EGFR_10	GRCh37/hg19	chr7	55224452	55224525	+
EGFR_11	GRCh37/hg19	chr7	55225356	55225446	+
EGFR_12	GRCh37/hg19	chr7	55227832	55228031	+
EGFR_13	GRCh37/hg19	chr7	55229192	55229324	+
EGFR_14	GRCh37/hg19	chr7	55231426	55231516	+

Supplementary Table S2. Summary of molecular data from the ISH and sequencing analyses conducted on both the pre-treatment primary tumor and the liver biopsy obtained after progression on panitumumab plus vemurafenib treatment. List of abbreviations: IHC, immunohistochemistry; ND, not done; SISH, dual-color silver in-situ hybridization; FISH, fluorescence in-situ hybridization.

	Pre-treatment tumor sample	**Post-treatment tumor sample**
MET IHC	H-score 150	H-score 270
MET SISH	18% amplified cells	85% amplified cells
MET FISH	16% amplified cells	75% amplified cells
HER-2 IHC & SISH	Negative	Negative
Next-generation sequencing*	BRAF V600E (allelic frequency 27%) SDHD I40V (allelic frequency 44%)	BRAF V600E (allelic frequency 14%) SDHD I40V (allelic frequency 57%) No additional mutations

*Based on the percentage of mutant reads, both pre-treatment and post-treatment tissue samples displayed substantially comparable tumor purity.